MEMORANDUM FOR: Themis Speis, Director
Division of Safety Technology

NOV 18 1985

FROM: O. E. Bassett, Director
Division of Accident Evaluation

SUBJECT: STEAM EXPLOSION ENERGETICS

A recent letter to you from Dr. T. G. Theofanous on Steam Explosion Energetics suggested a "peer review process and feedback" and a presentation at a one day meeting some time after the middle of December.

The enclosed copy of the draft summary chapter from LANL's report on "An Investigation of Steam Explosion Loadings with SIMMER-II" provides several interesting examples for comparison with Dr. Theofanous's examples. One point of great interest will be the amount of venting calculated, given an explosion in the lower plenum. Currently these two reports calculate significantly different amounts of venting, but under different initial conditions because of the examples selected.

Given the importance of this topic, we suggest a simultaneous peer review process for both reports and presentations by Dr. Theofanous and LANL at a two day meeting with time allowed for peers to provide their reviews and development of an overall consensus. Recall that some early results from the LANL work were presented at the Steam Explosion Review Group Meeting in Harpers Ferry. The final draft of the LANL report is expected to be ready for review by the first week in December. A simultaneous review process will save contractor and staff time, and travel costs.

We suggest that three weeks be allowed for review of both reports beginning December 16, 1985. Considering the Christmas Holidays taken at many national laboratories, we suggest the two day meeting be held about January 15, 1986. For meeting arrangement and coordination responsibilities, we suggest Mr. Cardis Allen and Mr. John Telford.

Please let me know whether you agree with these suggestions.

O. E. Bassett, Director
Division of Accident Evaluation

Enclosure: As stated

cc: Harold Sullivan, LANL
Charles Bell, LANL
William Bohl, LANL
distribution: circ; chron; [redacted]; Curtis; Kelber; CAllen; Ross; Minogue; Morrison; Bassett

FOIA-86-678
6/7

OFC:	CSRB	: CSRB	: DD:DAE	: D:DAE	:	:
NAME:	TELFORD/lm	: CURTIS	: MORRISON	: BASSETT	:	:
DATE:	11/14/85	: 11/14/85	: 11/15/85	: 11/15/85	:	:

259

DRAFT

AN INVESTIGATION OF STEAM EXPLOSION LOADINGS WITH SIMMER-II

by

W. R. Bohl

Contributors

C. R. Bell
T. A. Butler
L. M. Hull
J. G. Bennett
P. J. Blewett

DRAFT

TABLE OF CONTENTS

ABSTRACT .....
LIST OF FIGURES .....
LIST OF TABLES .....
I. SUMMARY REPORT .....
A. Introduction .....
B. Modification of SIMMER-II .....
C. Calibration to SNL Steam Explosion Experiments .....
D. Calibration to Los Alamos Shallow Pool Experiments .....
E. SIMMER-II Reactor Case Calculative Results .....
F. Containment Failure Probabilities .....
G. Conclusions and Recommendations .....
II. SIMMER-II MODIFICATIONS FOR THE MOLTEN-CORE/COOLANT INTERACTION PROGRAM.
A. Introduction .....
B. Summary of Modified Equations .....
1. AEOS Modifications .....
2. Heat Transfer Modifications .....
3. Vaporization-Condensation Modifications .....
C. Discussion of AEOS Modifications .....
1. Review of Difficulties in the Manual Formulation .....
2. Examination of Proposed Solutions to AEOS Problems .....
3. The Vapor Heat Capacity Modification .....
4. Modification of the Gas "Constant" at High Pressures .....
5. Definition of the Vapor Temperature for Single-Phase Cells and Other Modifications .....
6. Discussion of Results .....
7. Suggestions for Further Improvement .....
8. Conclusions .....
D. Modification of SIMMER-II Liquid-Liquid Heat Transfer for Water ...
E. Vaporization/Condensation Model Changes .....
F. Miscellaneous Corrections for the Molten-Core/Coolant Interaction.. Program .....
III. LOWER HEAD MODEL FOR SIMMER-II .....
A. Introduction .....
B. Input .....
C. Head Failure .....
D. Lower Head Motion .....

E. Boundary Conditions and Edits .....
F. Correction Set .....
G. Sample Problem .....
IV. CORRELATION TO SNL STEAM EXPLOSION EXPERIMENTS .....
V. ANALYSIS OF LOS ALAMOS EXPERIMENTAL DATA FOR SHALLOW POOLS .....
A. Introduction .....
B. Experimental Correlation .....
C. Hypothetical Cases with Nonuniform Interfaces .....
D. Experimental Comparison with a Pressure Ratio of 50:1 .....
E. Experimental Comparison with a Nonuniform Initial Interface .....
F. Conclusions .....
VI. ANALYSIS OF STEAM EXPLOSIONS WITH SIMMER-II .....
A. CASE 1 .....
1. Water Surface Area Investigation .....
2. Comparison to the ZIP Study Using the New Models .....
3. Case 1 Update .....
B. CASE 2 .....
1. Explosion After 1 second of Mixing (Scoping Calculation) .....
2. Explosion After 0.7 s of Mixing (Second Scoping Calculation) .
3. Case 2 Finalized .....
C. CASE 3 .....
D. CASE 4 .....
E. CASE 5 .....
VII. PROBABILITY OF A STEAM EXPLOSION .....
VIII. RESEARCH PRIORITIES ON STEAM EXPLOSIONS .....
APPENDIX A: THE SIMMER-II MANUAL ANALYTIC-EQUATION-OF-STATE TREATMENT .....
APPENDIX B: CFS NODE /VAPOR/WRBAEOS (EQUATION OF STATE CORRECTION SET).....
APPENDIX C: REVISED SIMMER-II INPUT DESCRIPTION FOR THE AEOS .....
APPENDIX D: AEOS SIMULATION PROGRAM .....
APPENDIX E: SUGGESTED VALUES FOR WATER AEOS INPUT .....
APPENDIX F: STANDARD SIMMER-II LIQUID-LIQUID HEAT-TRANSFER MODEL .....
APPENDIX G: CORRECTION SET FOR MODIFIED LIQUID-LIQUID HEAT TRANSFER .....
APPENDIX H: VAPORIZATION/CONDENSATION CORRECTION SET .....
APPENDIX I: SIMMER-II MANUAL TREATMENT OF THE VAPORIZATION/CONDENSATION MODEL .
APPENDIX J: MISCELLANEOUS CORRECTIONS .....
APPENDIX K: SUMMARY DESCRIPTION OF THE HEAD FAILURE MODEL SUBROUTINE .....
APPENDIX L: DEFINITIONS OF VARIABLES IN THE PLUGW CORRECTION SET .....
APPENDIX M: LOWER HEAD DYNAMIC ANALYSIS .....

APPENDIX N: CONSIDERATIONS REGARDING RESULTS FROM THE SDOF FAILURE MODEL .....
APPENDIX O: A LIMITED REVIEW OF SNL STEAM EXPLOSION EXPERIMENTS .....
APPENDIX P: SIMMER-II INPUT FOR THE MD-19 EXPERIMENT USING A UNIFORM MIXING ZONE
APPENDIX Q: SIMMER-II COMPARISON WITH THREE FIELD MIXING CALCULATIONS .....
APPENDIX R: SIMMER-II INPUT FOR THE ANALYSIS OF THE MD-19 EXPERIMENTS USING A NON-UNIFORM MIXING ZONE .....
APPENDIX S: EFFECT OF CHANGING THE AXIAL AND RADIAL CONSTRAINTS IN THE SIMULATION OF MD-19 .....
APPENDIX T: EXPLOSION CALCULATION STARTING WITH A STANDARD SIMMER-II PREMIXED CONFIGURATION .....
APPENDIX U: SIMMER-II PREMIXING WITH HIGH STEAM PRODUCTION RATES .....
APPENDIX V: DETAILS ON THE UPPER BOUND SIMMER-II STEAM EXPLOSION CALCULATION ..

DRAFT

AN INVESTIGATION OF STEAM EXPLOSION LOADINGS WITH SIMMER-II

by

W. R. Bohl

Contributors

C. R. Bell
T. A. Butler
L. M. Hull
J. G. Bennett
P. J. Blewett

ABSTRACT

The SIMMER-II code was used to provide estimates of the maximum anticipated loads on the upper head of a pressurized water reactor (PWR) following an in-vessel steam explosion. The SIMMER-II equation of state and heat-transfer models were upgraded for this purpose. A calibration to SNL steam explosion data and a comparison with Los Alamos shallow-pool experiments was performed. A lower-head failure and motion model was developed. Analysis of parametric cases suggests that the upper bound on the conditional probability of alpha-mode failure, given core melt, should be 0.01 if the vessel upper head and bolts are near normal operating temperatures. Suggestions are made for activities that could lead to increased confidence in the understanding and quantification of steam-explosion issues.

I. SUMMARY REPORT

A. Introduction

The purpose of this work was to provide a reasonable estimate of the maximum loads that might be expected at the upper head of a pressurized water reactor (PWR) following an in-vessel steam explosion. Using the determined range of loads, judgments were to be made on the potential for containment failure by missile production resulting from a steam explosion, commonly called alpha-mode failure, assuming core melt has occurred.

The calculations of loads were performed by the SIMMER-II code. A previous study of this type, herein called the ZIP study[1], was performed in 1980. To provide some basic SIMMER-II capabilities lacking in the 1980 study, a brief program of code modification was undertaken as part of this work. These modifications are discussed in Sec. B. To calibrate the revised modeling to available steam explosion experimental data, Sandia National Laboratories (SNL) intermediate-scale thermite-water experiments were assessed, and one particular well-characterized experiment, MD-19, was calculated with SIMMER-II. This discussion is in Sec. I.C. Evaluation of the adequacy of the SIMMER-II post-explosion expansion dynamics was investigated by comparing calculations with scaled shallow pool experiments. The experiments and the analysis performed are given in Sec. I.D. As the study proceeded, numerous scoping calculations on a full-scale PWR representation were performed; the results of these calculations are in Sec. I.E. These reactor results were integrated into an overall scheme for judging the containment failure probability, presented in Sec. I.F. Finally, conclusions and recommendations from this study are given in Sec. I.G. To keep the volume of this summary chapter from being excessive, most of the above outlined sections will present summary material only. Details are given in subsequent chapters of this report.

B. Modification of SIMMER-II

The SIMMER-II code was modified to better represent a corium-water system, and to implement a lower head failure and motion model suggested by the ZIP study. The details of these changes are given in Chaps. II and III and Appendixes A to N.

The four major areas of code modification for treating the corium-water system are an improved equation of state (EOS), a more appropriate nonequilibrium heat transfer to low thermal conductivity liquid water, revised assumptions in the vaporization-condensation model regarding energies at which water is vaporized and condensed, and miscellaneous changes.

---

[1]M. G. Stevenson, "Report of the Zion/Indian Point Study, Volume II," Los Alamos National Laboratory report LA-8306-MS, NUREG/CR-1411 (1980).

The most significant EOS modification in terms of accuracy was to make the infinitely dilute, water-vapor heat capacity temperature dependent, which better represents the increasing degrees of freedom of the water molecule and the hydrogen-oxygen system at high temperatures. For 3000 K infinitely dilute steam, the new heat capacity relationship gives 1.62 times the value for infinitely dilute 400 K steam.

The major modification to the EOS in terms of coding was to insert a relaxation constant so that as steam becomes more superheated its internal energy becomes closer to the value for infinitely dilute water vapor. This is most important for stability because it limits the triple-valued nature of the vapor temperature as a function of density. It is also important for accuracy, removing a spurious pressure dependence for superheated steam, as well as allowing the inclusion of the ~830 kJ/kg energy difference that appears between steam at the critical point and infinitely dilute steam at the critical temperature.

A fitting procedure was applied to the new EOS relationships to compare them with both the Steam Tables[2] and the Los Alamos SESAME tables.[3] Agreement is within ±20% over the range of interest and generally is much better. Given the phenomenological uncertainties in steam explosions, these results exceed the required accuracy. The main conceptual problem remaining (the one that relates only to the EOS) is a better variation of the gas parameter, R, near the critical point and at high steam density and temperature.

The SIMMER-II heat-transfer problem with the corium-water system relates to the low thermal conductivity of water. As a consequence of model development based on liquid sodium, the standard SIMMER-II code transfers heat to bulk liquid, which then vaporizes. For water, both experiments and theoretical considerations support the view that steam-explosion liquid-liquid heat transfer occurs to the water surface. Some heat then is conducted into the water; the remainder causes vaporization. Implementation of this revised concept allows

---

[2]J. H. Keenan, F. G. Keyes, P. G. Hill, and J. G. Moore, Steam Tables (New York, John Wiley and Sons, 1978).

[3]Kathleen S. Holian, Ed., "T-4 Handbook of Material Properties Data Bases, Vol. 1c: Equations of State," Los Alamos National Laboratory report LA-10160-MS (November 1984).

simulation of steam explosions in water-rich systems with nonequilibrium vaporization.

The radiation heat-transfer regime occurring during the coarse premixing phase of a steam explosion was not modeled explicitly. Bounding cases that envelop a variety of heat transfer modes and magnitudes were evaluated instead. Modeling a film boiling flow regime with radiation and film layer conduction in these chaotic environments is beyond the scope of the SIMMER-II formalism at this time and would add only marginal improvement to the overall treatment by itself. The lack of physics for fuel stream breakup and water interpenetration of the fuel are probably more important deficiencies in the SIMMER-II code.

We found that inclusion of water subcooling into an effective heat of vaporization was necessary to obtain reasonable results from the revised heat transfer model. Past experience has suggested that the complementary process, putting vapor superheat into the effective condensation energy, also would be desirable. Although conceptually straightforward, these changes did result in somewhat complex coding modifications.

The miscellaneous changes involved programming the liquid water thermal conductivity as a function of temperature, changing the maximum water droplet size algorithm, inserting an additional time-step control for the vapor energy work term, and correcting of two minor FORTRAN coding errors.

The necessity for treating structural effects can be introduced with the observation that only energetic steam explosions are a concern in evaluating containment failure. These energetic explosions could cause a rupture in the lower vessel head area that could be expected to mitigate upwardly directed kinetic energy significantly.

Finite element calculations indicated that vessel failure could be expected at the radius where the outermost vessel penetrations are located. A circumferential split would be expected to proceed around the head at this radius and leave the inner portion of the head as a free body. A simple, single-degree-of-freedom spring-mass model was correlated to these finite-element results. This model accepts the average pressure loading over the failure region and furnishes the time and downward head velocity when the head disengages from the vessel.

Motion of the head segment into the lower vessel cavity was treated by a modification of the SIMMER-II plug ejection model. The failed portion of the lower head becomes a free body whose acceleration is computed from its mass and the integrated forces acting on it. A two-dimensional representation of the cavity was used in this study; the volume available to the venting materials assumed the below core cavity was half filled with water.

C. Calibration to SNL Steam Explosion Experiments

The selection of SIMMER-II input parameters for use in reactor steam explosion analysis can best be accomplished with reference to the experimental data base. Two difficulties exist. First, any SIMMER-II model will be simplistic. The ability to propagate a mechanistic fragmentation (detonation) wave leaving behind a distribution of particle sizes does not exist in the code. In fact, a generally agreed upon theoretical fragmentation mechanism does not exist for steam explosions. Second, the reported experiments have random aspects. Later experimental results have tended to contradict earlier experiments and especially contradict early simplistic theories. Also, the experimental information is sufficiently ambiguous that any unique simulation is impossible. Because of these problems, one typical experiment was selected for computational simulation using a simple SIMMER-II representation. Details for this calibration as well as a brief review of SNL steam explosion data are given in Chap. IV and Appendixes O to T.

The experiment selected was SNL test MD-19,[4] where 5.11 kg of iron-alumina thermite was dropped into 224 kg of ambient temperature water contained in a square Lucite box. Initially, a uniform interaction zone of a size reported by the experimentalists was used. It was reported to have a thermite/steam/water volume ratio of 0.04/0.48/0.48. A two-phase, equal volume fraction steam/water chimney was assumed to exist above the interaction zone. The bottom of the box was assumed rigid. The sides and top of the box were assumed to be at constant pressure. These lateral boundary conditions assume the Lucite has no strength. Alternative boundary conditions are discussed in Appendix S.

---

[4]D. E. Mitchell, M. L. Corradini, and W. W. Tarbell, "Intermediate Scale Steam Explosion Phenomena: Experiments and Analysis," Sandia National Laboratories report SAND81-0124, NUREG/CR-2145 (1981).

Best results in the SIMMER-II simulation were achieved by having a water droplet size at a fractional multiple of the fuel droplet size. This was assumed to be reasonable because water surface tension is about an order of magnitude lower than that of iron-alumina thermite or corium. However, the fit was less than satisfactory, with a spurious high-pressure tail resulting from bulk heating of water in the interaction zone.

A second fit then was made using a previously calculated fuel/water distribution based on a three-velocity-field film boiling model.[5] Here the outline of the calculated mixing zone was correlated to the vague pre-explosion experimental configuration. The node with the peak thermite density had a thermite/steam/water volume fraction of 0.27/0.37/0.36. The best fit achieved was with a fuel particle diameter of 300 μm, a water droplet diameter of 75 μm, and a liquid-liquid heat transfer multiplier of 0.2. (Note that the new liquid-liquid heat transfer model was used with the 0.2 multiplier. This multiplier only acts on heat transfer to the water surface.) A comparison to the base pressure transducer is shown in Fig. 1.

The final exercise using SIMMER-II was to perform some pre-explosion coarse-mixing calculations, with initially separated thermite and water. Although the functional forms of some of the physics modeled in SIMMER-II is less than desired, obtaining an appreciation of the qualitative errors involved was desirable. These results will be used in Sec. I.E in running bounding cases for the reactor meltdown problem. The first calculation was to assume a uniform 15-mm droplet size with the nominal (unmodified) SIMMER-II heat transfer model. Steam production and the extent of thermite dispersion were underestimated. This calculation was rerun with the heat transfer models of Sec. I.B. Excessive radial thermite dispersal resulted, and the interaction zone did not reach the bottom of the Lucite container in the required time. The configuration established with the first premixing calculation was exploded with the same models and parameters used in the fit shown in Fig. 1 to see the effect of different premixing on the characteristics of the explosion. The peak pressure increased to 20.8 MPa, there was a longer time at high pressure, but the width of the pulse at 8 MPa was about the same. These results are consistent with

---

[5]W. R. Bohl, "A Calculational Advance in the Modeling of Fuel-Coolant Interactions," Proceedings of the L. M. F. B. R. Safety Topical Meeting, Lyon France, American and European Nuclear Societies, pp. III-557 to III-566 (1982).

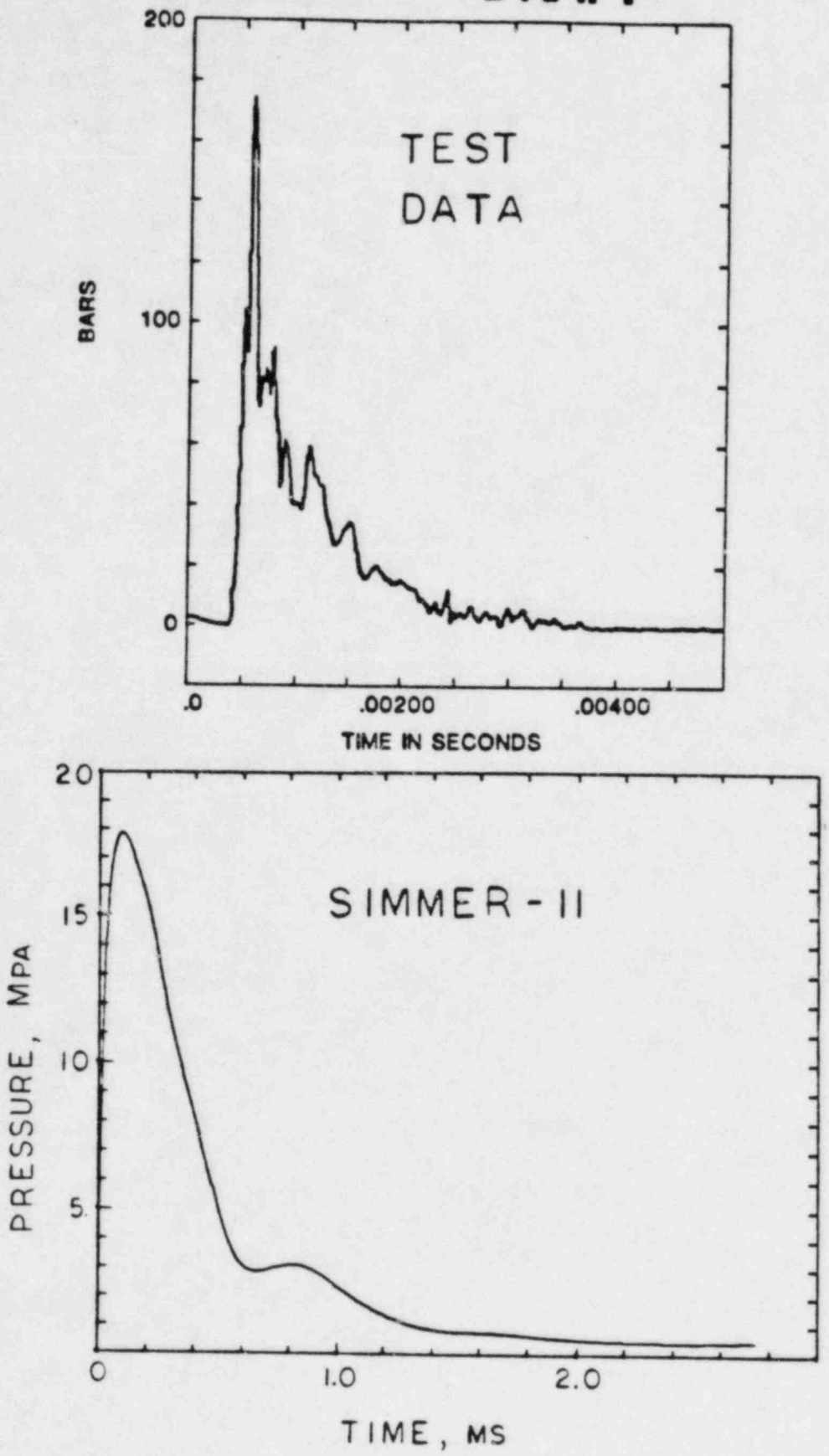

Fig. 1.

Comparison of water chamber base pressures in experiment MD-19.

what would be expected with less local vapor volume for early expansion and therefore pressure reduction. Although the calibration exercise was unable to provide a strongly supported, unique set of calibration parameters, it did provide some confidence that the SIMMER-II treatment was qualitatively reasonable. Also, knowledge was obtained on the choices of parameters that would envelop the real behavior.

As a caveat, details from other FITS experiments, such as double explosions or significantly more efficient explosions through the use of rigid walls, cannot be modeled mechanistically with SIMMER-II. Parametric studies coupled with additional model development are required to provide high confidence that consequences of all possible steam explosion phenomena are included in any study.

D. Calibration to Los Alamos Shallow Pool Experiments

To investigate a basis for judgments on the ability of SIMMER-II to calculate post-explosion slug breakup, a series of shallow pool acceleration experiments were conducted and then analyzed with SIMMER-II. Details of these experiments and their analysis are provided in Chap. V.

A schematic of the test apparatus is shown in Fig. 2. The depth of the pool and the height of the free space above the pool are scaled using the actual reactor vessel dimensions and the total amount of fuel available. As indicated in the schematic, a very thin (0.006-mm) diaphragm supports the pool in a 102-mm-i.d. Plexiglas tube. The pool is 50 mm deep, and there is 185 mm of free space above the pool. The bottom of the tube is separated from the nitrogen driver gas by a 0.1-mm Mylar diaphragm. The experiment is started by cutting the lower diaphragm; the pressure rises in the bottom tube and ruptures the thin diaphragm that supports the water. The increased pressure then induces the motion of the water that is of interest. Three sets of data are collected during the test: the pressure history just under the top diaphragm (P1), the pressure history at the endplate (P4), and a high-speed movie. Although some random behavior was observed, the results of these tests are still interesting.

Three types of SIMMER-II calculations were performed, simulating both real and hypothetical experiments in this geometry. These were (1) calibration cases relating to one experimental test, (2) hypothetical cases with postulated curvature in the thin Mylar diaphragm supporting the pool, and (3) calculative comparisons with other shallow pool experiments using the calibrated parameters.

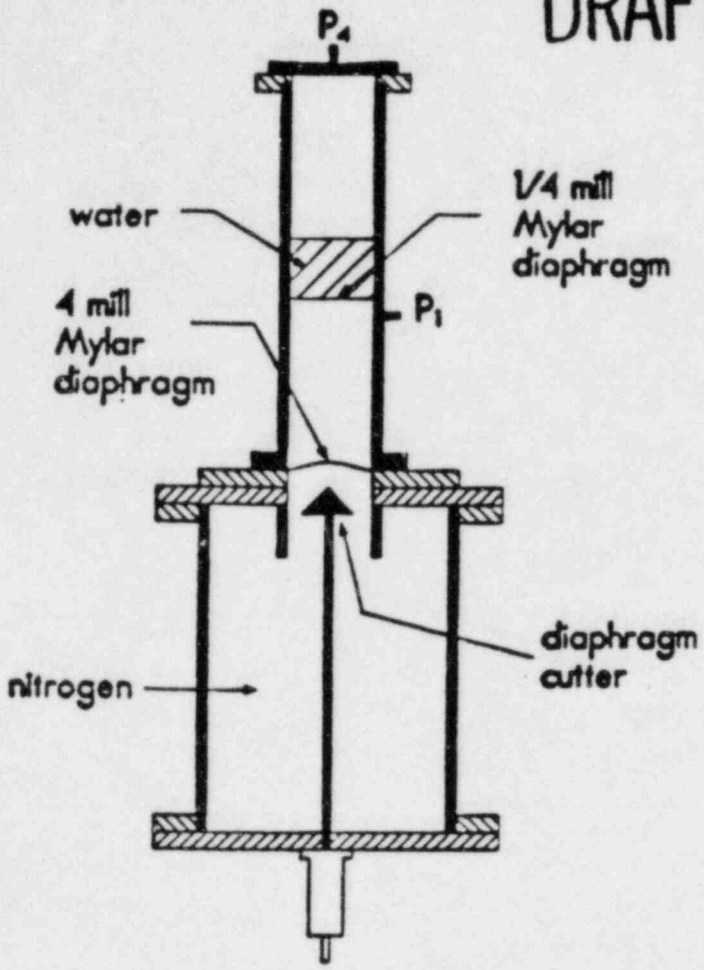

Fig. 2.
Shallow pool experimental apparatus.

For the calibration cases, the initial nitrogen driver gas pressure was 0.56 MPa, and the evacuated space started at ~5.6 kPa. Consequently, these tests are referred to as having a 100:1 pressure ratio. The high-speed movies indicated progressive slug breakup as a function of distance, with complete breakthrough occurring at about the time of endplate impact. A reasonable simulation of the experimental pressure trace was obtainable in SIMMER-II by using a small drop diameter, 100 μm, and consequently maintaining close coupling between the liquid and vapor fields. Also, the value of α_0, the vapor volume fraction where the two-phase to single-phase transition occurs, was adjusted to 0.025 to attempt to maintain two-phase pressures as long as possible upon impact. The best comparison with experimental data is shown in Fig. 3.

Two types of hypothetical situations were examined. First, the inner one-half of the lower water interface area was raised or lowered 1 cm to evaluate the efforts of surface shapes on pool breakup. Second, one of these nonuniform situations was scaled to up by a factor of 40 to evaluate the

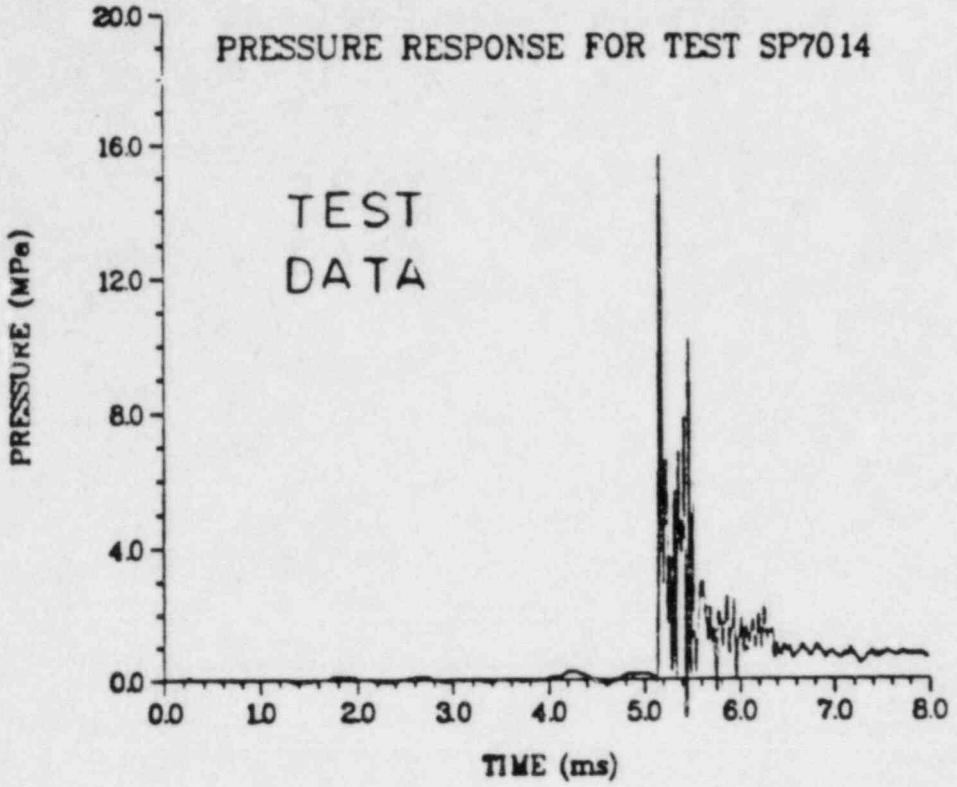

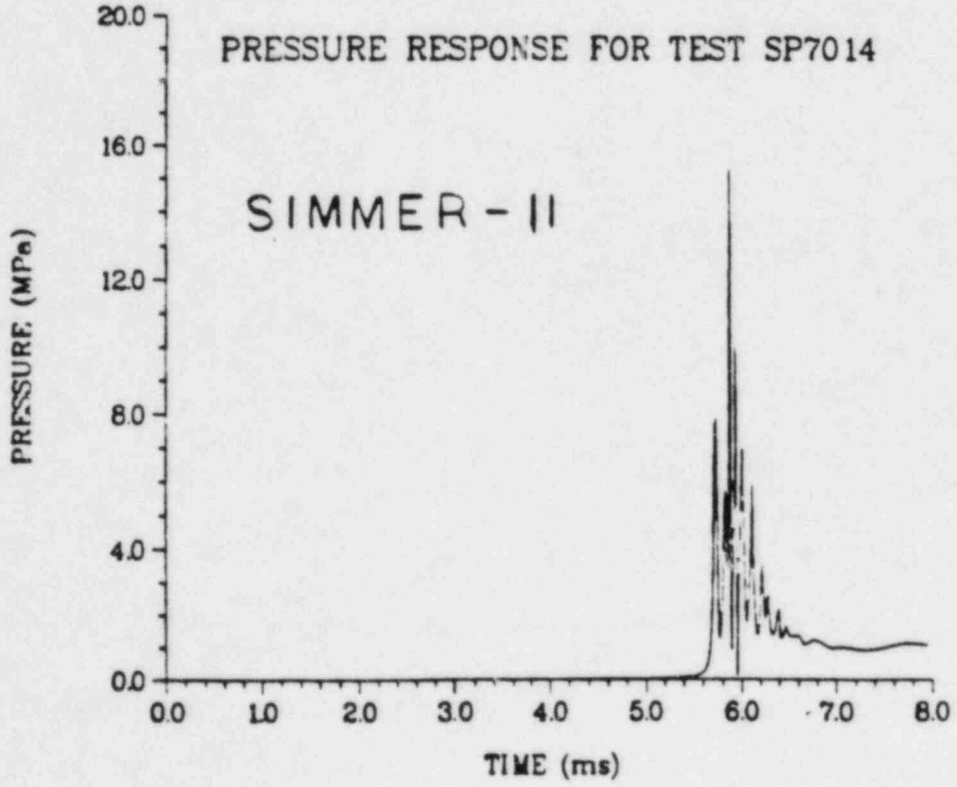

Fig. 3.

Comparison of P4 pressures in the shallow pool experiments.

scalability of the treatment. The nonuniform interface resulted in an instability growth that definitely made impact appear as more of a two-phase spray, but actual venting of the gas through the water was not achieved. A further calculation with half of the distorted lower interface actually blocked by a rigid disk was performed to assess an experimental concept for testing the effects of interface distortion. The results suggested that the qualitative difference of the pool behavior was not changed significantly by the disk. Therefore, a distorted interface experiment was planned. Increasing the scale (and driving pressure) did produce the expected increase in peak impact pressure by a factor of 40, but the upscaled case resulted in a more coherent impact.

The two remaining calculations made in comparison to experiments were (a) one with a 50:1 pressure ratio and (b) one with a depressed lower pool interface by a central disk. The impact pressure for the 50:1 case, which was obtained with the "calibrated" parameters, had peaks more than twice than measured. The character of the 50:1 calculation was much like that at 100:1. Although slug breakup in the high-speed movie of the 50:1 experiment was similar to that for the 100:1, a significantly more diffuse impact is implied by the pressure trace. With a disk to lower the center of the lower water interface by 3 cm, both the experimental and the calculation showed gas breakthrough before impact. However, now the calculative impact was significantly more diffuse than that measured.

The following conclusions were reached in this brief SIMMER-II examination of shallow pool dynamics.

(a) The SIMMER-II simulation of shallow pool breakup provides generally correct global behavior in terms of diffuse vs slug impact and overall impulse delivered by the fluid to the upper closure. It can not, and probably need not, match the very short duration pressure spikes measured in the experiments.

(b) With an initially uniform pool, the use of small drops in SIMMER-II probably would exaggerate upper head loadings in the reactor case (be conservative).

(c) Even with exaggerated liquid-vapor coupling, the lack of a model for turbulent mixing leads SIMMER-II to overly accelerate slug breakup in the case where small nodes are used to simulate a nonuniform interface in this experiment.

(d) Because the node size at reactor scale is much larger than the turbulent mixing length, exclusion of a turbulent mixing model appears justified. Also, the non-linear scaling of the SIMMER-II liquid-vapor drag relationship was a major contributor in increasing impact coherence of the upscaled calculation.

(e) Because of unresolved scaling questions, further analysis of these experiments was judged less cost effective than parametric calculations involving reactor meltdown sequences.

E. SIMMER-II Reactor Case Calculative Results

The range of uncertainty in the expected conditions resulting in a steam explosion during a core meltdown is large[6]. If all possible initial conditions and modeling uncertainties were considered, a complete parametric study of steam explosions and their effects would be an enormous effort. The effort involved in even one SIMMER-II reactor calculation is appreciable. With the limited scope of this study, the limited understanding of steam explosions that exists, and the limited extent to which this understanding currently has been programmed into SIMMER-II, a massive parametric study was not appropriate. Rather, five scoping calculations were performed with SIMMER-II to address the upper bound question. Details of these calculations, as well as some additional results that help to integrate these cases into the context of a meltdown accident sequence are given in Chap. VI and Appendixes U and V. The results are summarized in this section.

The reactor structural representation for these cases is shown in Fig. 4. The in-vessel configuration is the same as in the previous ZIP study. A movable

---

[6]M. Berman, D. V. Swenson, and A. J. Wickett, "An Uncertainty Study of PWR Steam Explosions," Sandia National Laboratories report SAND83-1438, NUREG/CR-3369 (1984).

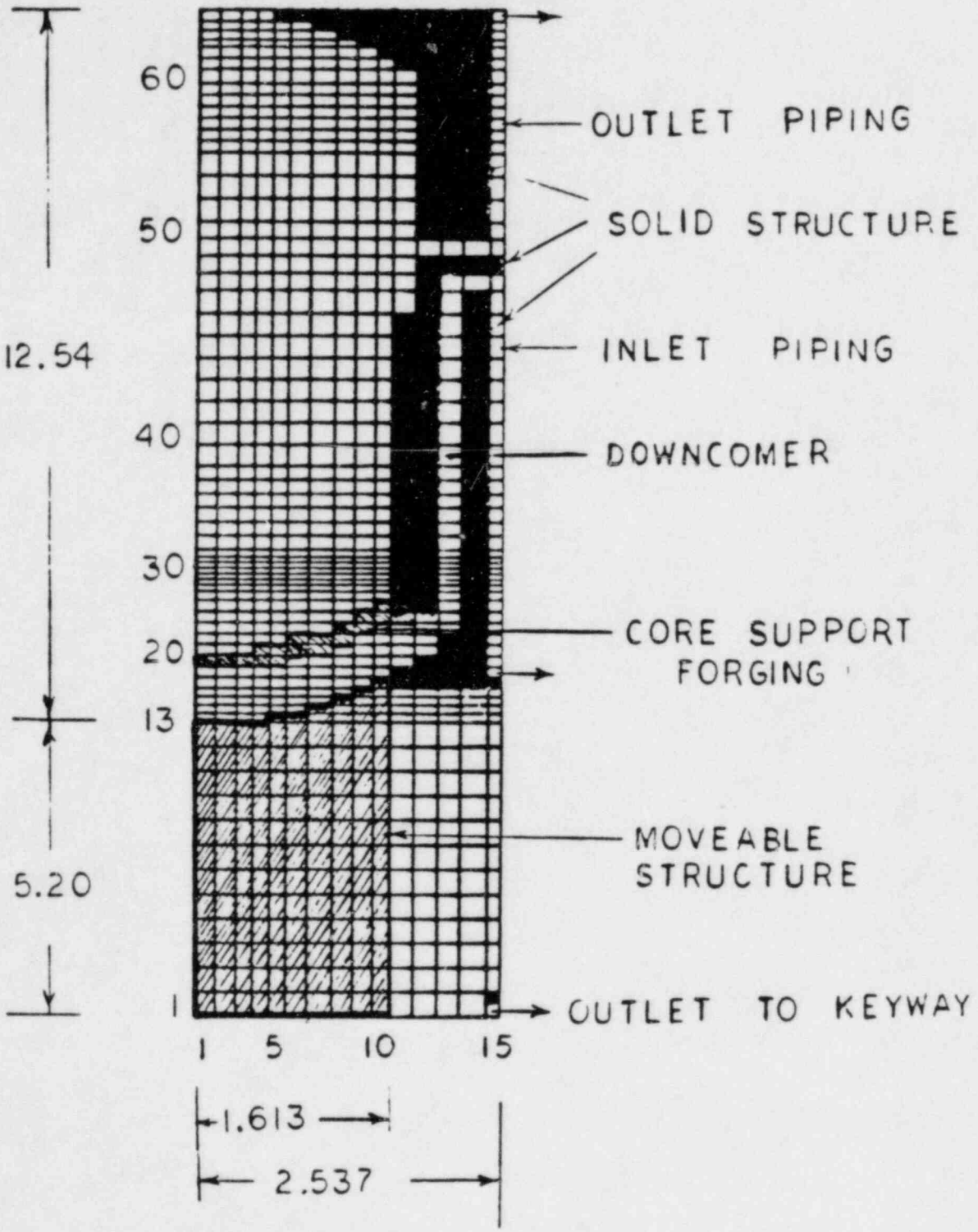

Fig. 4.
PWR structural representation for SIMMER-II steam explosion calculations

lower structure has been added for the lower head failure model. The five SIMMER-II cases can be summarized as follows.

In case 1, we used the same SIMMER-II corium and water geometry as in Cases 1 and 2 of the 1980 ZIP study. This was a premixture comprising 20% of the total corium below a single-phase molten corium pool. The corium/steam/water volume fractions were 0.50/0.25/0.25. The fuel and water were assumed to be fragmented to 300-μm-diam globules within the premixture. In addition, 35 000 kg of steel particles were added between axial node 46 and node 60 to represent the mass, but not the strength, of the upper core structure for this case. The new SIMMER-II lower head failure, equation of state, and heat transfer models were used.

The results of the calculation indicated a substantial reduction (compared with the ZIP study) in the likelihood of energetic missile production. The new models eliminated the spurious high-interaction-zone, single-phase pressures previously obtained. Lower head failure was calculated to occur at 3.5 ms, and about 57% of the kinetic energy was directed downward as a result. Upwardly directed kinetic energy at head impact was ~650 MJ. With the assistance of the downward venting of core material following lower head failure, the peak force on the head was reduced from 2.6 GN (giganeutons) to 1.0 GN. A plot of the integrated upper head loading is shown in Fig. 5. This head loading is near the thresbold for failure if the head is near the normal operating temperature.

In case 2, we used more mechanistic but arguably conservative initial conditions for a large-scale coherent steam explosion. Starting with a completely molten core at 3100 K, a 1.85-m-diam corium stream was allowed to pour into 18 000 kg of water in the lower plenum. Standard SIMMER-II heat transfer was used with 20-mm-diam, prefragmented corium globules. Based on the results in Sec. I.C, these assumptions should underestimate steam production and thereby permit extensive mixing. Mixing occurred around the edges of the corium stream, and was reasonably extensive because of large mesh size used (greater than 10 cm).

An explosion of the mixed corium and water was triggered 0.7 s after initiation of the pour, when 40 000 kg of corium had entered the lower plenum and corium flow reversal was starting as a result of vapor production and plenum pressurization. This time was chosen because the mixing configuration appeared to have the potential to produce maximum head loads. Examining details of timing sensitivity was beyond the scope of this study, but an explosion after

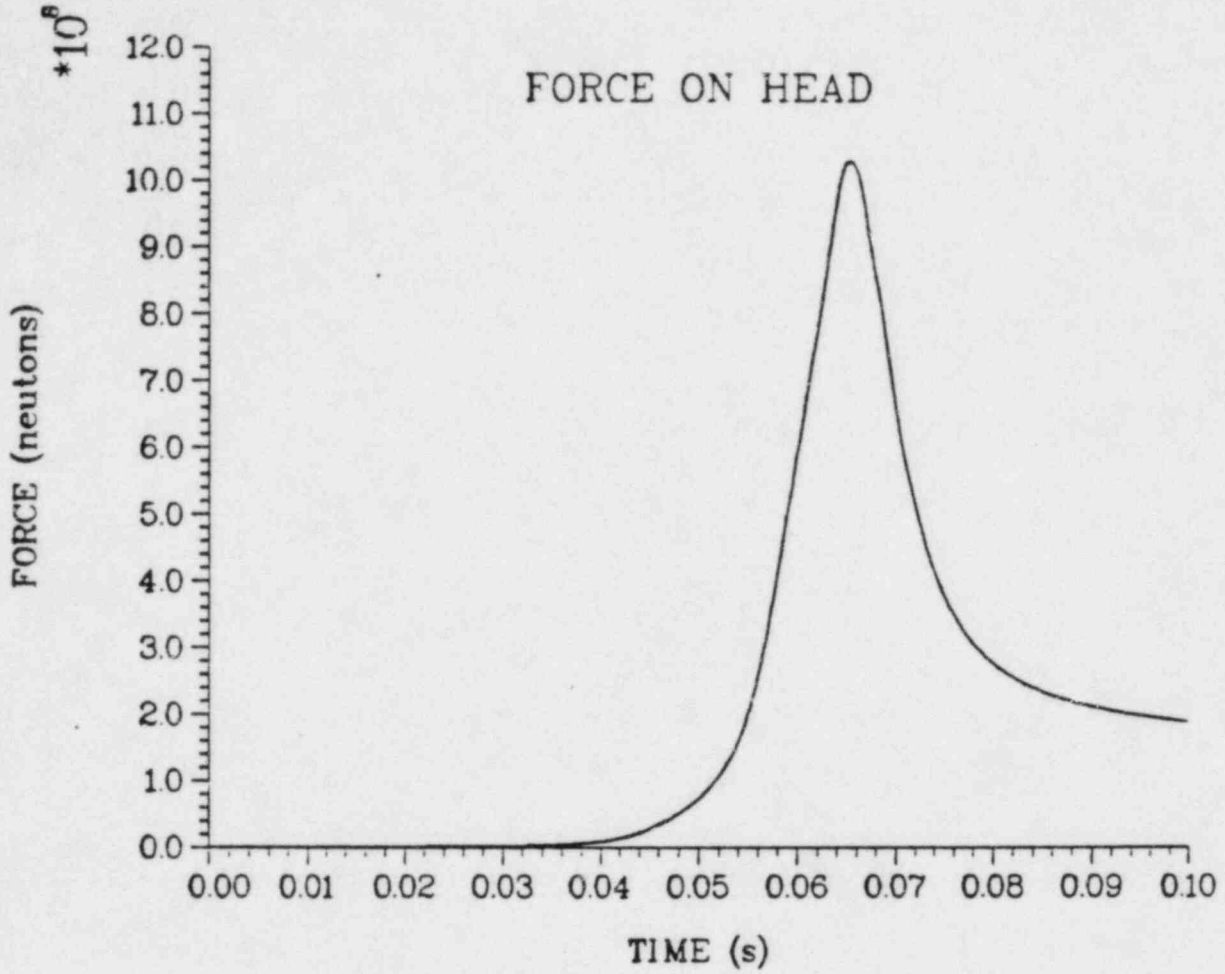

Fig. 5. Integrated upper head loading for case 1.

1 s of mixing is discussed in Chap. VI. The SNL calibrated explosion parameters were used with the new SIMMER-II models. Steel particles were included to represent the upper internal structure. About 62% of the kinetic energy was directed downward. Upwardly directed kinetic energy at heat impact was ~500 MJ. The peak upper head force was 0.81 GN, as shown in Fig. 6.

In case 3, we used worst-case initial conditions as inferred from a recent SNL study[7]. Here 75% of the core (94 000 kg) was assumed to mix with 20 000 kg of water. To limit the height of the premixture to that of the original corium pool, a 19% initial steam volume fraction was assumed. The corium globule size was assumed to be finely fragmented to 100 μm in diameter. although the new

[7] Ibid.

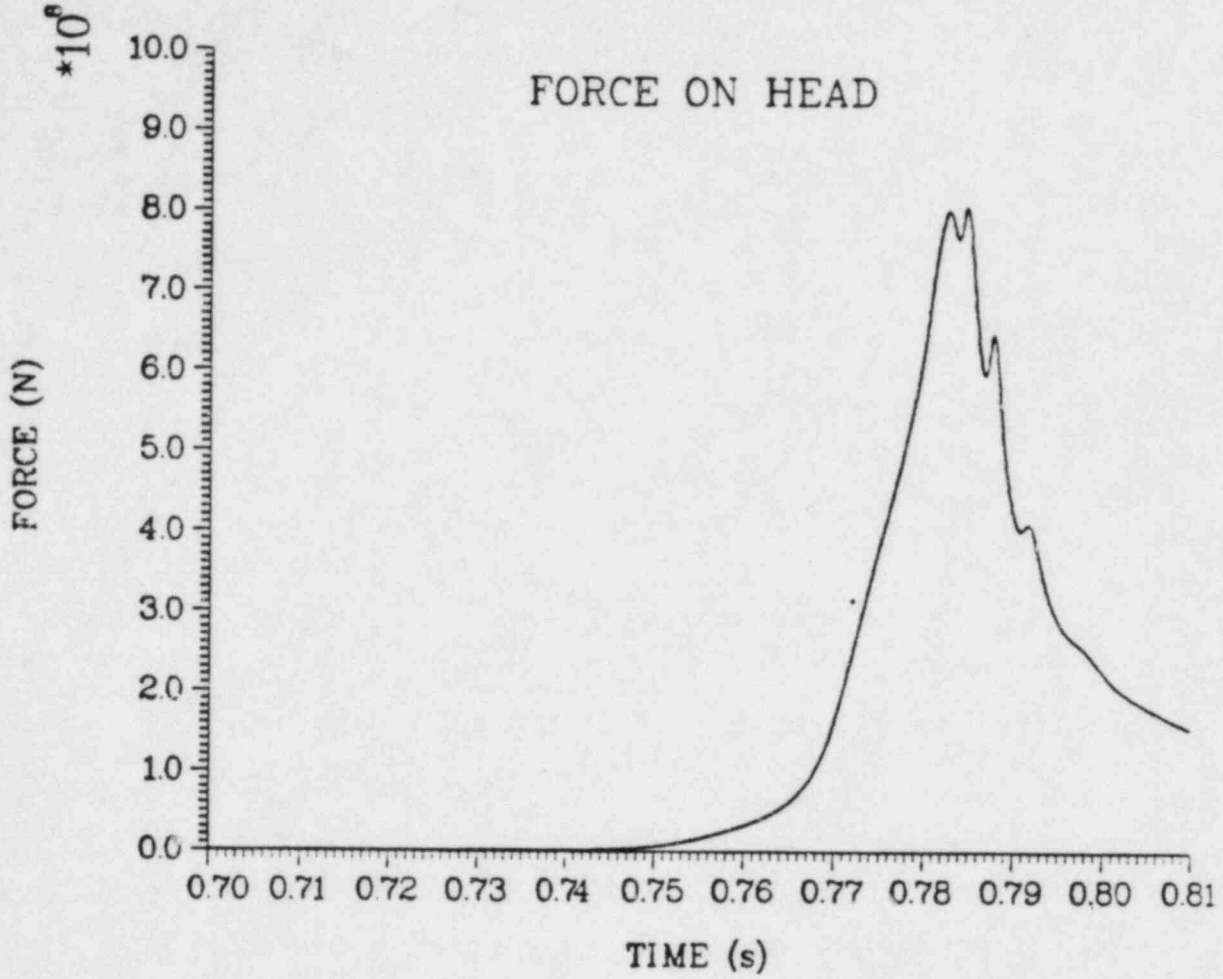

Fig. 6. Integrated upper head loading for case 2.

SIMMER-II models were used, no heat transfer from frozen corium to steam was calculated, limiting steam temperatures during the expansion to 922 K. No lower head failure was assumed, and the remaining core material and upper structure was assumed not to inhibit expansion. The upwardly directed kinetic energy was 1830 MJ. However, as a consequence of the diffuse nature of the expansion, the peak upper head force was only 0.78 GN, as shown in Fig. 7. This result shows that a complex relationship exists between the explosion and its delivered loads to the system. Simple correlations are not reliable.

In case 4, we took the initial conditions from case 2 but homogenized the 40 000 kg of corium and 10 000 kg of water in the lower plenum. A slow "explosion" then was simulated where droplet sizes were increased an order of magnitude over the SNL correlated values. This reduces the heat transfer rate by 2 orders of magnitude. The idea was to simulate an incoherent, multiple

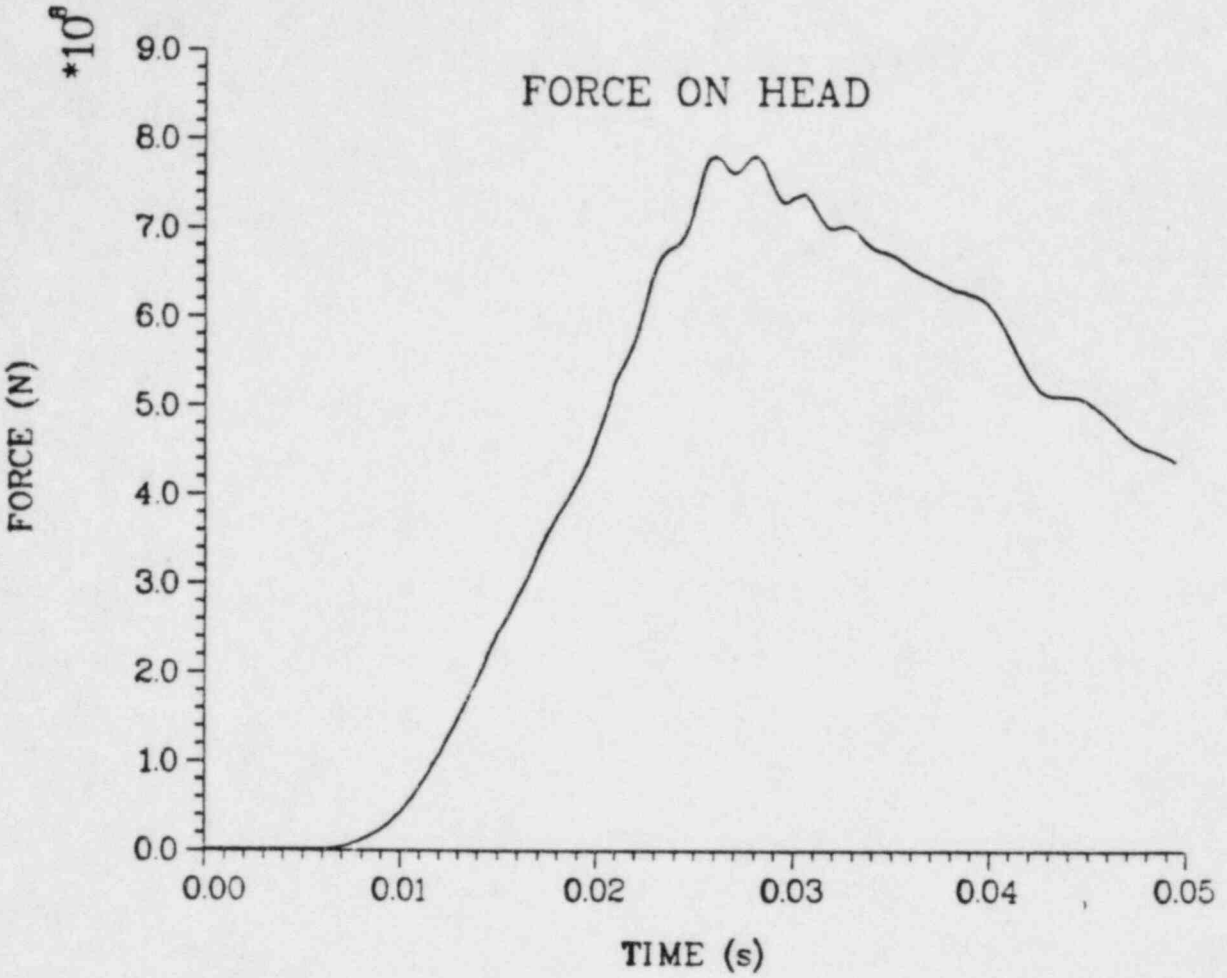

Fig. 7. Integrated upper head loading for case 3.

explosion environment that could be more representative of the reactor situation. In case 4, the lower plenum was not calculated to fail. Upwardly directed kinetic energy at heat impact was ~760 MJ. The peak upper head force was 1.52 GN, as shown in Fig. 8. This case had a significantly more coherent upper head impact than cases 1, 2, or 3, even though the explosion was relatively benign. Again, the complexity of relating explosion magnitudes and characteristics to loads on the head is evident. Here the most benign explosion produced the largest challenge to the head.

In case 5 we used the case 3 premixture but with corium and water thermally equilibrated before the expansion. The Low Alamos SESAME tables were used to give a starting pressure of 900 MPa. Refitted parameters for the SIMMER-II EOS were derived to obtain these initial conditions. The remaining 25% of the core was placed on top of the premixed region. Both lower head failure and steel

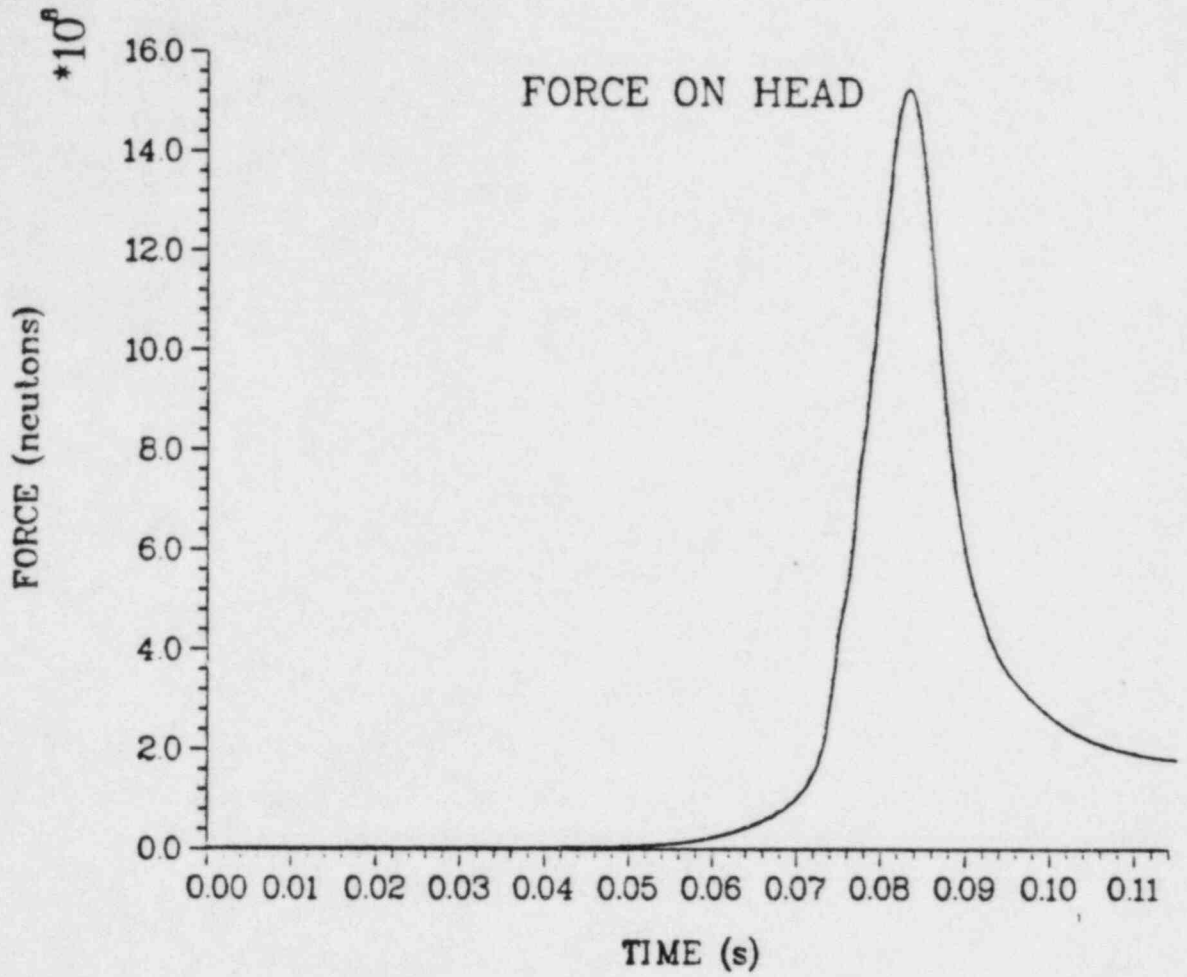

Fig. 8. Integrated upper head loading for case 4.

particles (for structure) were included in the calculation. The maximum upwardly directed kinetic energy was 7250 MJ. The peak upper head force was 12.4 GN, which was obtained just before the calculation went unstable. The force plot is shown in Fig. 9. This result confirmed clearly that our calculated approach would produce the expected diasterous results for the upper limit assumptions and idealized physics.

F. Containment Failure Probabilities

To obtain an estimate for the probability of containment failure from an in-vessel steam explosion, given core melt, we must (a) judge how likely the initial conditons for a large scale steam explosion are, (b) estimate the in-vessel energetics and loadings produced by the spectrum of possible steam

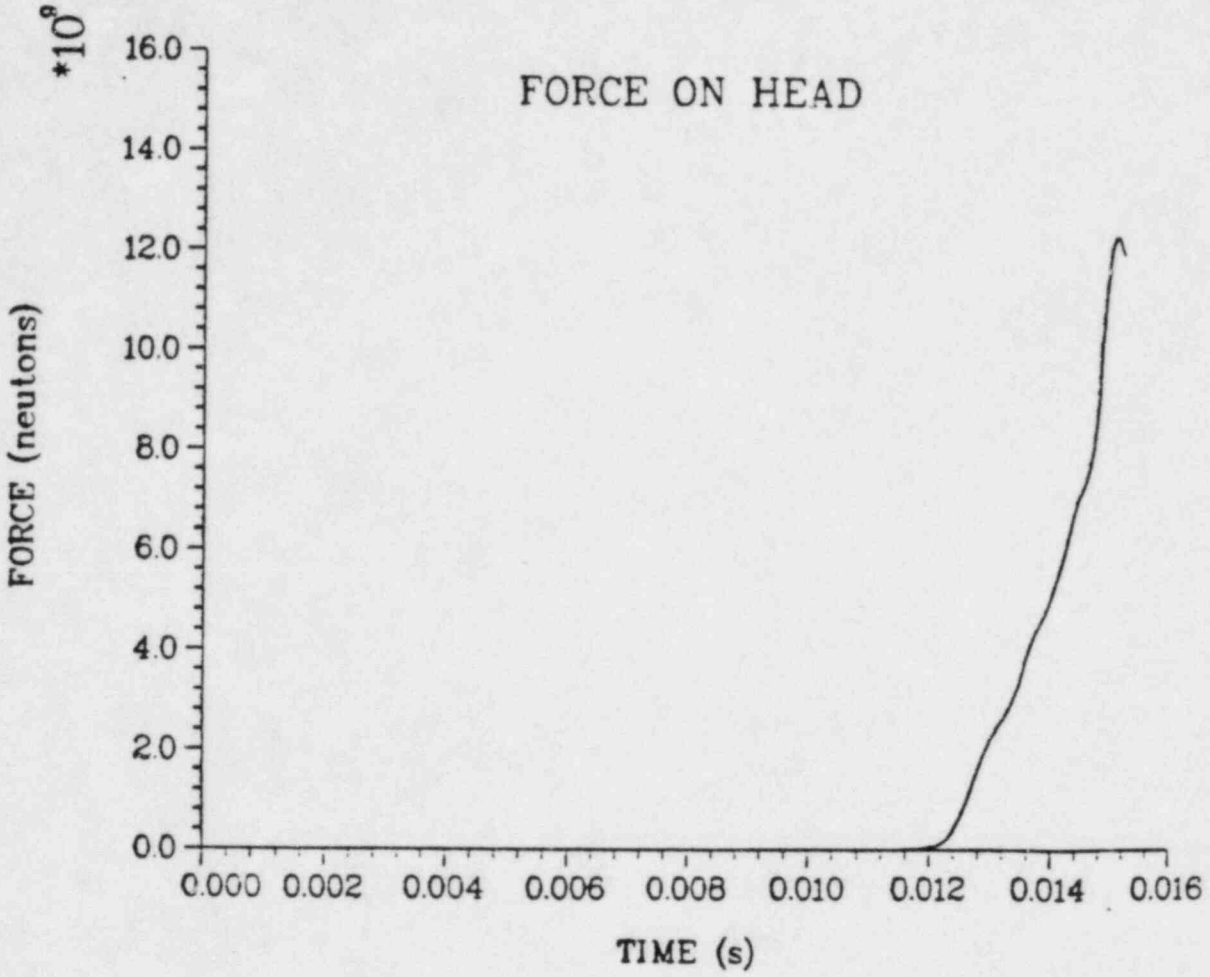

Fig. 9. Integrated upper head loading for case 5.

explosions, and (c) evaluate the consequences of such loadings. A brief study attempting to make such judgments is presented in Chap. VII. Here we summarize some conclusions from that study.

First, although the best-estimate probability is judged to be low (between 10^{-3} - 10^{-4}), this is simply a guess. We currently lack the technology to construct a reliable probability density function for core melt consequences that would portray a best-estimate or most probable value. Indeed, performing any "best-estimate" mechanistic core meltdown calculation, with models representing consensus phenomenology, was not possible because consensus phenomenology did not exist. The SIMMER-II calculations performed were for addressing the upper bound question.

Second, any large-scale steam explosion or sequence of explosions leading to a containment challenge apparently must involve a sustained supercritical pressure. Although IDCOR aserts the maximum meaningful pressure during the expansion phase of an explosion is about half the thermodynamic critical pressure,[8] steam explosion experiments exist with expansion phase pressures greater than 34 MPa sustained for more than 1 s.[9] Thus, containment challenge from large-scale steam explosions cannot be ruled out on the basis of limited pressures.

Third, with the dissipation calculated by the SIMMER-II model, to obtain sufficient energy a large-scale steam explosion apparently must involve efficient energy transfer from a considerable fraction of a molten core, 20% or more, in a few tens of milliseconds. This leads to such requirements as forming a large molten corium pool, having a coherent pour, not obtaining early triggering of an explosion, and limiting steam generation so as to permit the extensive premixing of corium and water. All of these are unlikely, but not outside the spectrum of reason. For example, triggering could be delayed by saturated water or elevated ambient pressures or the commonly quoted steady-state fluidization arguments, which limit mixing, could be defeated by the inertial effects involved in a large corium pour. Because of the edge-of-spectrum character of these phenomena, a 0.1 probability was judged to be a proper upper limit to associate with obtaining initial conditions resulting in sufficiently energetic steam explosions. Further explanation as to the meaning of this probability value is in Chap. VII.

Fourth, obtaining the extreme conditions presented in case 5 appears to be impossible. Mixing 75% of the core requires water to rise through a molten corium pool in a film boiling regime because of the necessity to accommodate the vapor volume produced. In any meaningful calculation attempting to attain this premixed configuration, satisfaction of fluidization requirements resulting in

---

[8]Fauske and Associates, Inc. "Technical Report 14.1A, Key Phenomenological Models For Assessing Explosive Steam Generation Rates," The Industry Degraded Core Rulemaking System (IDCOR) (1983).

[9]K. H. Wohletz, Los Alamos National Laboratory, Private Communication. Some background on these experiments can be found in Michael F. Sheridan and Kenneth H. Wohletz, "Hydrovolcanism: Basic Considerations and Review," Journal of Volcanology and Geothermal Research 17, 1-29 (1983).

corium dispersal would be assured. The assumptions of instantaneous temperature equilibration and pessimistic equation-of-state parameters are also unreasonable. Case 5 merely demonstrates that if arbitrary mixing is allowed, and the explosion efficiency is allowed to approach the thermodynamic limit, SIMMER-II obtains the expected unacceptable result.

Fifth, if the vessel head is to become a large missile, an integrated threshold head loading of approximately 1 GN is required if the head and bolts exist at the reactor operating temperature. Case 2, run with edge-of-spectrum initial conditions for a single large explosion, was below this level. Case 1 produced 1 GN, although its postulated premixing as well as its explosion/expansion sequence involved edge-of-spectrum considerations. Case 4 achieved more than 1 GN. However, true multiple explosions are not calculated. The initial conditions are idealized (for example, with uniform material distributions radially), dissipation of energy in the upper core structure is neglected (with 900 MJ of fluid kinetic energy, this could be significant), and the time-dependence of the nonuniform upper head loading suggests formation of multiple missiles from the head apex, which could be stopped by the missile shields. In brief, case 4 is an edge-of-spectrum expansion calculation. Because of the end-of-spectrum character of calculations exceeding 1 GN, if the head and bolts exist at operating temperature, a 0.1 probability is judged appropriate for obtaining vessel loadings of concern given initial conditions resulting in energetic steam explosions.

Sixth, any attempt to establish a simple limit condition is fuzzy. An impulse limit is useful only if the impact involves single-phase liquid. Case 3 shows that high energies do not necessarily give unacceptable loads, if a highly two-phase spray is the impacting fluid. The 1 GN force limit is fuzzy because of the influence of the spatial loading distribution, the temperature of the vessel, and the response of the containment to any missile. Head loadings depend on the assumptions made in the explosion/expansion calculations. In this study, the presence of steel particles tended to concentrate loads, while lower head failure made upwardly directed impacts less severe. Thus, consistent analysis must be performed that links initial conditions, mixing characteristics, explosion characteristics, expansion behavior, head failure characteristics, and missile dynamics.

G. Conclusions and Recommendations

This study has resulted in significant progress over the ZIP analyzes. The SIMMER-II water EOS and heat-transfer mechanics are more credible. The significance of lower-head failure can be evaluated consistently and shown to result in considerable mitigation for the constrained (by the corium pool) reactor meltdown case. The initial conditions used for a steam explosion can be related to a mixing calculation. Although SIMMER-II models can only parametrize the physics of steam explosions, the correlated models can now obtain a respectable pressure pulse for the experimentally observed water-rich system. Further, parameters can be chosen to provide a calculational simulation of shallow pool behavior. The use of steel particles for upper structure reduces fluid breakup and dispersal which were nonconservative in the ZIP analyses.

Because of the edge-of-spectrum character of both the calculative assumptions leading to a large scale stream explosion and those required to obtain significant head loading, the upper limit for the containment failure probability given core melt appears to be 10^{-2}, if the upper vessel head and bolts exist near ~550 F. For higher temperatures this probability must be increased. The importance of the high loadings in case 4, obtained from slow heat transfer simulating incoherent explosions, cannot be ignored. A method to quantify a true best-estimate probability does not exist. Present guesses suggest values of 10^{-3} to 10^{-4} might be reasonable.

A detailed discussion of possible future research to obtain increased confidence on the steam explosion issue is presented in Chap. VIII. Beyond an extension of this study to better quantify the consequences of the calculated upper head loadings, the proper priorities for additional research on the alpha-mode failure issue are judged to be (1) modeling of the meltdown process, (2) large-scale steam explosion experiments with associated model development for test analysis, test interpretation, and reactor application, and (3) smaller scale experiments to address specific mechanisms. The reasons for this judgment are as follows.

1. Understanding meltdown behavior would help place the alpha-mode of containment failure in its proper perspective among other safety issues.

2. Both the state of any corium pool before contact with water in the lower plenum and the mode of contact depend on the meltdown sequence, which is uncertain.

3. The state of vessel internal structures as well as the temperature of the vessel head and head bolts depend on heat transfer during the core heatup (meltdown) phase of an accident.

4. Both SIMMER calculations[10] and the theories[11] of Corradini, Fauske, and Theofanous lead to the conclusion that large-scale explosions will possess characteristics that differ from the smaller scale FITS tests. These differences are sufficiently qualitative to be observable with current technology.

5. Ultimately, reduction of uncertainty in the vapor explosion field is believed only achievable by inclusion of increases in scientific knowledge, not in the performing of parametric studies.

Finally, a judgment has to be made as to what level of residual uncertainty is tolerable. Otherwise, the steam explosion issues will tend to remain open-ended.

---

[10]This is shown when the calculations for test MD-19 are compared to Case 2 of Sec. V. Further discussion is in Chap. VIII on research priorities.

[11]Norman A. Evans, "The Effect of Core Melt-Coolant Interactions on Severe Accident Risks in Light Water Reactors," in Proc. International Meeting on Light Water Reactor Severe Accident Evaluation, American Nuclear Society, 18.1-1 to 18.1-8 (1983).

SANDIA NATIONAL LABORATORIES
Albuquerque, NM 87185

Date: November 20, 1985

To: M. Berman, 6427

From: M. F. Young, 6425

Subject: Evaluation of Pressure Transducer Measurements in HEX and SHE Tests

1.0 Introduction

This memo is an evaluation of the pressure transducer measurements taken in the SHE (Straight High Explosive) and HEX (High Explosive) tests performed at the FITS facility at SNLA. These tests were performed to get data on reliability and reproducibility of pressure gage readings obtained during the FITS tests in the Steam Explosion Program. Several different gage types and mounting techniques were tested. An additional purpose was to check on the accuracy of calculations performed with the CSQII[1] two-dimensional hydrodynamics code to analyze the FITS data.

The HEX series of tests were done using a wooden mandrel 11 inches long and 4 inches in diameter wrapped with 11 turns of primacord as the pressure source. This mandrel was placed in a 22 inch ID steel cylinder filled with approximately 2 feet of water in tests 1 through 9, and in a 22 inch square lucite chamber, also containing 2 feet of water, in tests 10 and 11. The mandrel was positioned either with the top of the mandrel level with the water surface, (high mount) or with the bottom approximately 4.5 inches from the bottom of the tank (low mount). In all cases, the primacord was ignited above the water surface; for the low mount cases, a single strand of primacord went down through the water to the mandrel along the axis of the tank. Charge weights ranged from 120 grains[1] to 1000 grains; all charges were PETN except for the 1000 grain charge, which was RDX, a somewhat hotter explosive than PETN. Table 1.1 shows the actual test conditions in more detail.

---

1. 1 grain = 1/7000 lbm or 6.48 x 10^-5 kg

The SHE tests were begun with the intention of providing a more symmetric geometry that could be analyzed with CSQII, as the HEX tests were actually three-dimensional, with the primacord burning in a spiral around the mandrel. This burning pattern was shown to cause asymmetries in the pressure pattern around the tank[2], as well as being a difficult source to model with CSQII using the existing JCL equation of state for PETN. The SHE tests consisted of a single strand of PETN primacord along the axis of the steel tank, which was filled with 2 feet of water. The strand was again ignited above the water surface. The portion in the water was either 11 inches long (high mount) or 20 inches long (low mount). These tests are also shown in Table 1.1.

2.0 Evaluation

In general, although the SHE tests are geometrically symmetric, the consistency of gage response is not good in terms of pressure amplitude; the shapes of the pressure traces and arrival times are in good agreement, both between symmetrically placed gages and with CSQII results. Measured peak pressures also do not agree with CSQII predictions, being one-half or less of the calculated pressures. These results indicate that some problems exist with the gages, the principal candidates being tank vibrations coupling to the gages and gage resonance. Some characteristic times for the SHE and HEX test geometries are shown in Table 2.1.

The steel tank fundamental frequency, about 3kHz[3], has a time constant of 330μs, which is considerably longer than the SHE primacord burn time of 40μs; this, however, does not rule out tank vibration as a potential problem, since the fundamental frequency is that of free vibration and we are mostly interested in the transient vibrational response of the tank induced by shocks for this problem. The gage resonance is reported to be 700kHz, and the rolloff frequency of the data acquisition system at the FITS site is 50kHz. This latter frequency limit is due to the amplifier response. These frequency limits mean that any signal components with time constants shorter than about 20μs will be attenuated, and that gage resonance could be excited by signals with substantial components near 700kHz, or 1.4μs. Unfortunately, this is close to the rise time of the main explosion pulse in the SHE experiments (10μs).

Also shown in Table 2.1 are the transit times for various paths in the steel tank, plus the digitizer holdup time. This latter time should be added in when calculating arrival times for the pressure transducer locations.

Figure 2.1 shows the pressure trace from the lower wall position in SHE01. The high frequency hash visible just

before the first large peak and leading into it is a result of the gage responding to longitudinal vibrations carried through the wall. This hash appears to be a mixture of frequencies from 100-500kHz with amplitude ±50psi. Although this response is not terrible by itself and can be easily filtered out in this case, it does indicate that the gages will respond to wall vibrations. The strength and frequency of wall vibrations is a function of the forcing pressure (the explosion) and the location at which the vibration is measured. Thus, if the gages respond in this case, they may also respond at other frequencies and amplitudes for different explosion strengths. Figure 2.2 shows the overlaid pressure traces from the lower wall position in SHE05 and SHE06. SHE05 shows a pronounced 50kHz oscillation with amplitude ±500psi, probably gage resonance induced by the shock wave arriving through the water. Figure 2.3 is the same data after applying a lopass digital filter[4] to the original data (rolloff at 40kHz, 20dB down at 50Khz). Although the 50kHz signal is removed, there still appears to be an oscillation at about 25kHz. This latter cannot be removed effectively because it is of approximately the same frequency as the pulse and reflections from the explosive source in the SHE tests.

There is also some indirect evidence for gage resonance being a problem in the SHE tests in the form of many blown gages, although CSQII (and calculations assuming an inverse distance dependence for the pressure amplitude) indicate a maximum wall pressure of less than 4ksi, and the gages used are rated at either 5ksi, 10ksi, or 20ksi. The above implies resonance in the gages induced by the short rise time of the initial shock front in the water.

An example CSQII calculated pressure is shown in Figure 2.4 for the low wall gage position. Comparisons between Figures 2.2, 2.3, and 2.4 indicate that the CSQII predicted pressure is about 30% greater than that observed in the SHE tests on the first peak. The following reflection peaks are also higher.

The general conclusion that can be drawn from the SHE test data is that, although the SHE tests are geometrically symmetric, the source pulse is too fast for the instrumentation to respond, and in fact may cause destructive resonances in the gages. There may be some effect on the gages due to wall vibrations, but this is not clear from the evidence at hand. Such an effect can possibly be measured by using blocked-off gages, although this procedure will remove a possible coupling path from the wall to the gage through the water, as well as the direct source pressure.

3.0 HEX Tests

In the HEX tests, the total burn time is 580μs, giving a much wider overall pulse with a slower effective rise time of about 140μs. Since this wide pulse is actually made up of 11 overlapping narrow pulses from the 11 wraps of primacord, there are some irregularities present (see Ref. 2), and gages can still be blown, especially if they are located looking directly at the side of the mandrel. How uniform the pulse appears depends on the gage distance and orientation, both from the mandrel and from reflecting and free surfaces in the tank.

Figure 3.1 shows the data from HEX07 at the low wall position after first being filtered with a 50kHz lopass digital filter to remove high-frequency noise. The pulse clearly shows the structure consisting of the individual pulses from the primacord loops. Gage positions farther away and closer to the mandrel axis see more of a smeared pulse; that is, the individual pulses from the wraps overlap more. These smeared pulses tend to be more consistent from gage to gage and easier to interpret that those showing individual wrap pulses. Base-mounted gages generally see a very consistent pulse in the high-mount HEX tests. Figure 3.2 shows an overlay of three symmetric base gage positions from the HEX07 test, showing good agreement. High wall positions in the high mount tests generally see two distinct pulses, one from the source and a reflection from the base of the tank.

Table 3.1 contains the test number, gage location, peak pressure of the main pulse, and the impulse of this first pulse from HEX tests 1 through 7. Table 3.2 is the corresponding data from HEX tests 10 and 11 in which lucite was used as the water chamber. Missing gages in the two tables had experimental problems, such as loose wires, destroyed during the test, or very low readings compared to the other gages, indicating either blockage or an air bubble in the gage block. Some of the gages that are shown also exhibited problems (see notes in tables). The next table, Table 3.3, contains statistical data on the HEX tests for from two to four gages in symmetric positions. Gages not included either had problems or did not have a matching gage. The values shown are all for base gages, since at least one symmetric wall gage did not survive in each HEX test. The "±" numbers are the standard deviations, calculated using the estimated mean. The only two tests to be duplicated, 2 and 3, do not have the same pressures or impulses.

The pressures in the steel tank HEX tests, 1-9, are seen to have errors in the range ±4 to ±15%, depending on the test, with the corresponding impulses having errors in the range ±2 to ±11%. This level of accuracy is not apparent in the two HEX tests done in a lucite chamber, 10 and 11. An overlay of three symmetric base gage positions in HEX10 is shown in Figure 3.3. I would say that the agreement between the gages is nonexistent. Apparently, the walls are moving sufficiently over the duration of the pulse to affect the pressure at these gage positions, although, since we have only two tests to look at, a high mount and a low mount, further tests will have to be done to verify this hypothesis. What can be seen from the lucite chamber tests is that the pressures at similar gage locations are an order of magnitude lower in the lucite (free boundary) tests, than in the steel tank (rigid boundary) tests (see Figure 3.4). This points to the importance of considering system geometry and confinement when predicting pressure response at a given location.

4.0 Conclusions and Recommendations

As we have seen, the SHE tests have too fast a pulse for the instrumentation, and gages in the HEX tests can give different pulse shapes depending on gage location. A solution to these particular problems is to use a true slow-burning propellant as the pressure source; the resulting pulse should then be symmetric, with a pulse duration of around 1ms, and a rise time of around 250μs. This source will approximate the steam explosion source without the side effects of the primacord wraps in the HEX tests. The first test using this idea has been done in the steel tank and designated PRØØØ. The charge used consisted of 15 inches of M5-B propellant contained in a 2 inch ID PVC pipe, ignited with a pyrotechnic "rip" ignitor along the axis of the pipe. Results from this test are shown in Figures 4.1-4.4. The pressure traces are seen to be uniformly consistent, regardless of position or mounting. The first sharp pulse occurring at 0.5 ms is from the rip ignitor, not the main propellant charge. The main pulse traces, beginning at around 0.8 ms and lasting until 1.5 ms, show some structure differences due to echo and timing differences between gage location, but have envelopes that are very similar between all gage locations. The peak amplitudes, in particular, are virtually identical.

Another potential problem considered was the possibility of wall vibrations affecting gage response. For this reason, special isolation mounts were fabricated which hold the gages in frames weighted with lead bricks; the gages then poke through the tank wall and are sealed to the tank with

Silastic compound. It was felt that these mounts would remove any possible wall-to-gage coupling, except locally through the water itself. Comparison of isolated gages with wall-mounted gages in Figures 4.1-4.4 shows no significant difference, although there is slightly more spread in the wall-mount gage readings, and they are slightly higher, than the isolated gages. More tests will help to resolve these differences.

The poor consistency in the lucite tests will necessitate more tests, using propellant charges and isolated gages in the chamber sides. Possibly, the location of gage mounting will have to be re-examined for these tests; the British WUMT tests[5], for instance, have a similar, but not identical, design, and seem to give consistent pressure data.

One further item that should be considered in regard to steam explosions is the difference in behavior of explosive-type pressure sources as opposed to propellant-type sources resulting from the type of confinement. The basic difference is one of scale; explosives, at typical real-world scales, are said to detonate independently of confinement, although there is indeed an effect if the scale is small enough; propellants are said to burn and definitely are affected by confinement at real-world scales, although the effect disappears at large enough scale. The point of the above comments is that steam explosions take place with a characteristic time typical of propellants, not explosives; thus at FITS spatial scales, using 2-50kg of thermite, the efficiency of burning is probably a strong function of confinement. We can then expect efficiency to rise with increased confinement at this scale, as seems to be true in RC-2[6], but the effect should level out at some larger scale. We would, of course, like to know how large that scale may be, since we are ultimately interested in reactor size masses of corium and water.

5.0 References

1. CSQII Manual.

2. K. Schoenefeld, "Spiral Wrapping of PETN," Memo dated July 23, 1985.

3. W. Soedel, "A New Frequency Formula for Closed Circular Cylindrical Shells for a Large Variety of Boundary Conditions," Journal of Sound and Vibration, Vol 70, pp. 309-317 (1980).

4. S. Stearns, Digital Signal Analysis, Hayden Book Company, Inc., (1975).

5. WUMT Data Reports, AEE Winfrith.

6. M. Krein, "Estimation of the Conversion Ratio for the RC-2 Experiment," Memo dated May 17, 1985.

Table 1.1
Independent Parameters for all Tests

Test	Prima-cord (grains/ft)	Total Charge (grains)	Water Depth (inches)	Charge Location
HEX01	80	1000	24.0	High
HEX02	30	360	26.0	High
HEX03	30	360	26.5	High
HEX04	20	240	25.5	High
HEX05	20	280	24.0	Low
HEX06	10	120	25.0	High
HEX07	10	120	26.0	Low
HEX08	10	120	23.0	High
HEX09	10	120	24.0	Low
HEX10	20	240	25.0	High
HEX11	20	240	26.0	Low
SHE01	100	92	24.5	High
SHE02	100	167	24.5	Low
SHE03	100	92	24.0	High
SHE04	100	179	25.5	Low
SHE05	100	92	24.0	High
SHE06	100	92	24.0	High

Table 2.1
Characteristic Times in HEX-SHE Tests

Description	Distance (cm)	Time (μs)
18" Primacord in air[2]	45.7	70
11" Primacord in water (High)	27.9	43
20" Primacord in water (Low)	50.8	78
High mount SHE rise time	-	10
Digitizer holdup time	-	64
Tank center to wall[3]	28	156
Wall to wall	56	311
High SHE to Base Center	34.3	191
Low SHE to Base Center	11.4	63
Base Center to Base Inner	15.3	85
Base Center to Low Wall	30.7	171
Base Center to High Wall	60.2	334
HEX burn time	365.8	563
HEX rise time	-	141
High HEX to Base Center	46.9	261
High HEX to Base Outer	54.3	301
Gage Resonance	-	2 (700kHz)
Amplifier Rolloff	-	25 (40kHz)
Tank Fundamental Mode	-	330 (3kHz)

2. Detonation velocity = 6500m/s

3. Water shock velocity = 1800m/s

Table 3.1
Pressure and Impulse for Steel Chamber HEX Tests

HEX Test	WP/Type/Loc	Pressure (MPa)	Impulse (MPa-s)
01	1/FCP/BC//D	29.7 (flattop)	-------
	3/K/BNE/O/T	29.7 (flattop)	-------
	4/K/BSE/O/T	31.4 (flattop)	-------
	5/E/BNW/O/T	28.3	0.00644
	6/PS/WNE/U	17.9/31.7	0.00726
	7/E/BSE/O/D	30.0	0.00710
	10/E/BSW/O	27.9	0.00605
	11/K/WNE/L	37.2 (flattop)	-------
02	1/FCP/BC//D	-----	-------
	2/E/BNW/O/D	4.4 (bubble)	-------
	3/K/BNW/O/T	16.6	0.00445
	4/K/BSE/O/T	22.1	0.00440
	5/E/BSW/O/T	20.0	0.00446
	6/PS/WNE/U/T	6.2/9.0	0.00437
	7/E/BSE/O/D	17.9	0.00427
	11/K/WNE/L/D	55.2[4]	-------
03	1/FCP/BC//D	11.0/28.3 (flat)	-------
	3/K/BNE/O/T	22.8	0.00565
	4/K/BSE/O/T	23.4	0.00491
	5/E/BSW/O/T	25.5	0.00607
	6/PS/WNE/U/T	-----	-------
	7/E/BSE/O/D	22.1	0.00518
	11/K/WNE/L/D	37.9 (flat)	-------
04	1/PCB/BC//T	11.7	0.00382
	2/E/BN/I/D	12.4	0.00293
	3/K/BNW/O/T	13.8	0.00358
	4/K/BSE/O/T	18.6	0.00368
	5/E/WNE/L/D	10.3/24.1/13.8	0.00332
	6/K/WNE/U/T	-----	-------
	7/E/BSE/O/D	16.6	0.00346
	11/E/BS/I/T	(bubble)	-------

4. This gage, WP11, is a Kulite HKS-375, Serial No. 1090-8-10 5ksi range (34.5MPa). It flattopped in HEX01, is here reading twice its range, flattopped again in HEX03 and did not respond in HEX04. Evidentally broken.

Table 3.1 (continued)
Pressure and Impulse for Steel Chamber HEX Tests

HEX Test	WP/Type/Loc	Pressure (MPa)	Impulse (MPa-s)
06	1/PCB/BC//T	8.3	0.00291
	2/E/BN/I/D	13.1	-------
	3/K/BNW/O/T	14.8	0.00329
	4/K/BSE/O/T	14.8	0.00317
	5/E/WNE/L/D	10.8/12.6/7.9	0.00268
	6/E/WNE/U/T	4.5/12.4	0.00231
	7/E/BSE/O/D	13.8	0.00267
	11/E/BS/I/T	(bubble)	-------
07	2/E/BN/I/D	20.6	0.00375
	3/K/BNW/O/T	19.7	0.00373
	4/K/BSE/O/T	21.2	0.00386
	7/E/BSE/O/D	19.4	0.00343
	8/K/WSW/U	7.9 (low)	0.00063
	9/E/WSW/L	9.0/12.1/11.0	0.00274
	10/E/BN/I/T	19.3	0.00371

Nomenclature for WP/Type/Location in Table 3.1

The number is the WP channel number.

Under Type (first slash), PCB, FCP and PS are as shown, E means Endevco, and K means Kulite.

Under location (second slash), The first letter is either B (Base) or W (Wall). The letters after refer to the compass position (N = North, NW = Northwest, etc., and C = Center). The letter after the next slash is:

O = outer,
I = inner,
U = upper,
L = lower.

The letter (if present) after the last slash refers to gage orientation for gages mounted in a gage block: T = tee, D = direct.

Table 3.2
Pressure and Impulse for HEX Lucite Tests

HEX Test	WP/Type/Loc	Pressure (MPa)	Impulse (MPa-s)
10	1/PCB/BC//T	2.8	.000613
	3/K/BNW/O/T	1.2	.000187
	4/K/BSE/O/T	3.1	.000521
	6/K/WW/U	1.6	.000305
	7/E/BSE/O/D	0.7	.000122
	9/K/WE/L	2.2	.000130
11	2/E/BN/I	3.0	.000672
	3/K/BNW/O/T	4.1	.000774
	4/K/BSE/O/T	3.4	.000548
	5/E/WW/L/T	0.8	-------
	6/K/WW/U/D	19.3	-------
	8/E/WE/U/D	1.3	-------
	9/K/WE/L/D	4.3	-------
	11/E/BS/I/T	11.0	.001544

Table 3.3
Pressure Statistics for HEX Tests

HEX Test	Gages Averaged	Pressure (MPa)	Impulse (MPa-s)
01	4,5,7,10	29.40±1.6	.00678±.00066
02	3,4,5,7	19.1±2.4	.00439±.00009
03	3,4,5,7	23.4±1.5	.00545±.00052
04	3,4,7	16.3±2.4	.00357±.00011
06	3,4,7	14.5±0.6	.00304±.00033
07	3,4,7	20.1±1.0	.00367±.00022
	2,10	19.4±1.7	.00373±.00003
10	3,4,7	1.7±1.2	.00028±.00021
11	3,4	3.8±0.5	.00066±.00016

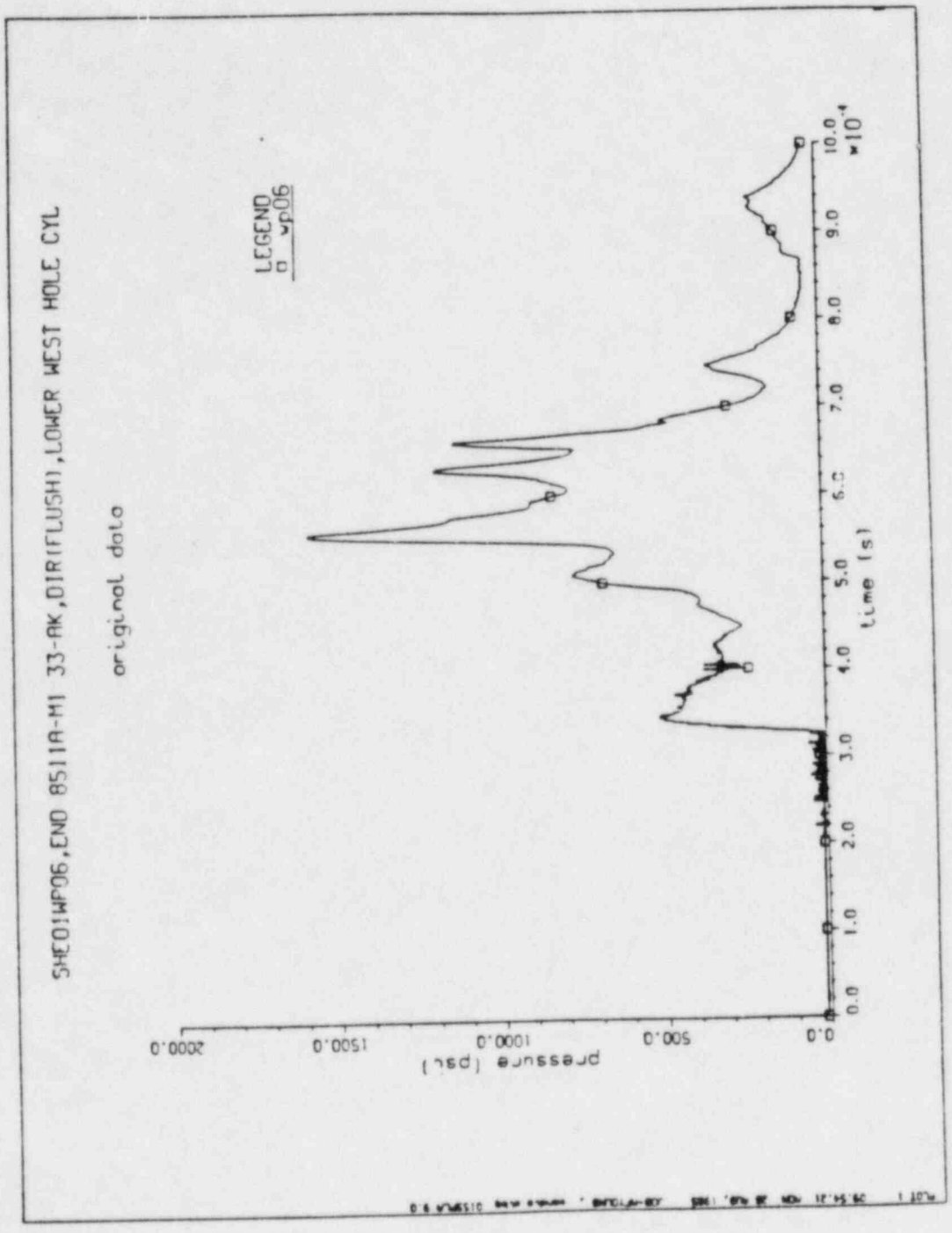

Figure 2.1 Unfiltered pressure trace from SHE01, lower west cylinder wall.

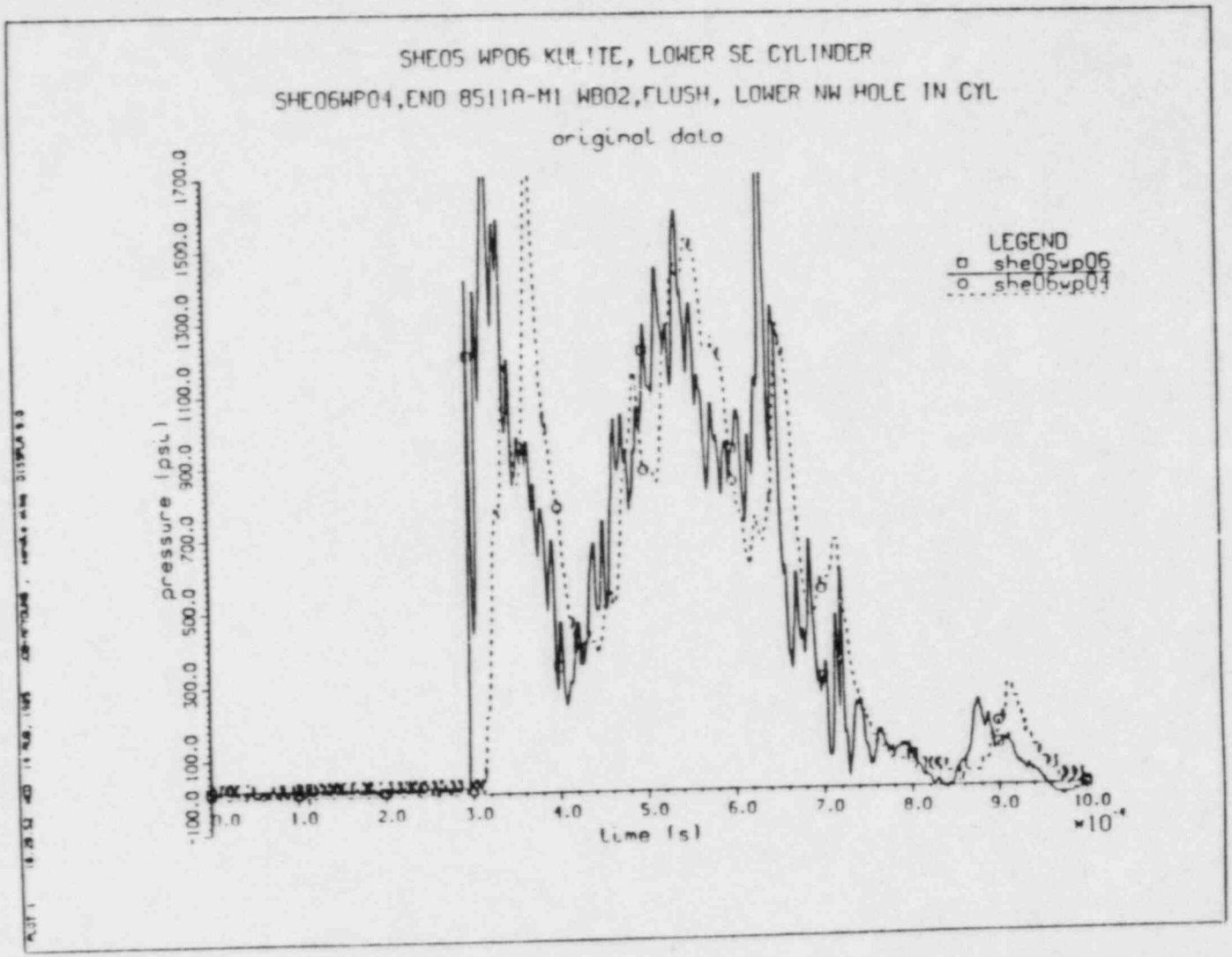

Figure 2.2 Overlay of unfiltered pressure traces from SHE05 and SHE06, lower cylinder wall position.

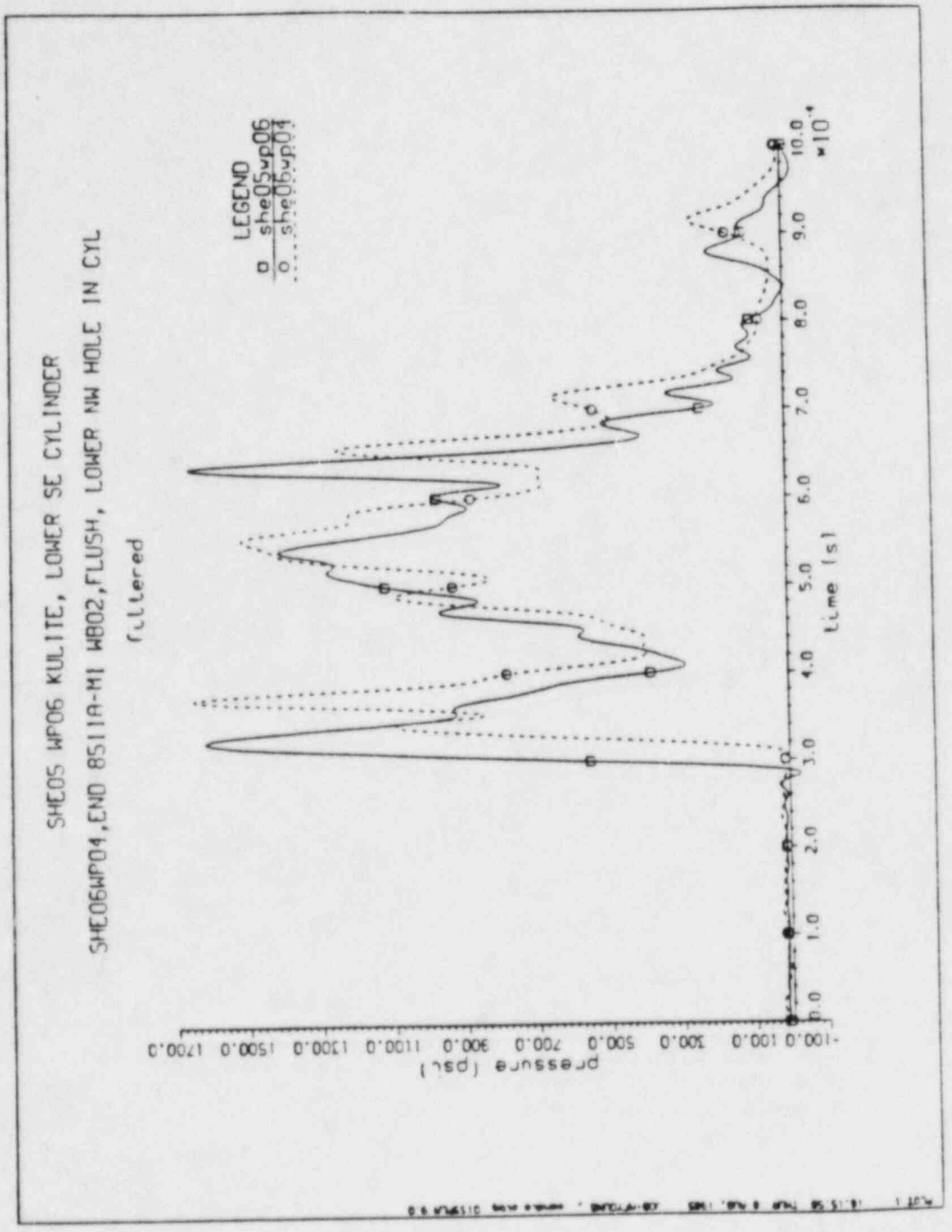

Figure 2.3 Overlay of filtered pressure traces from SHE05 and SHE06, lower cylinder wall position.

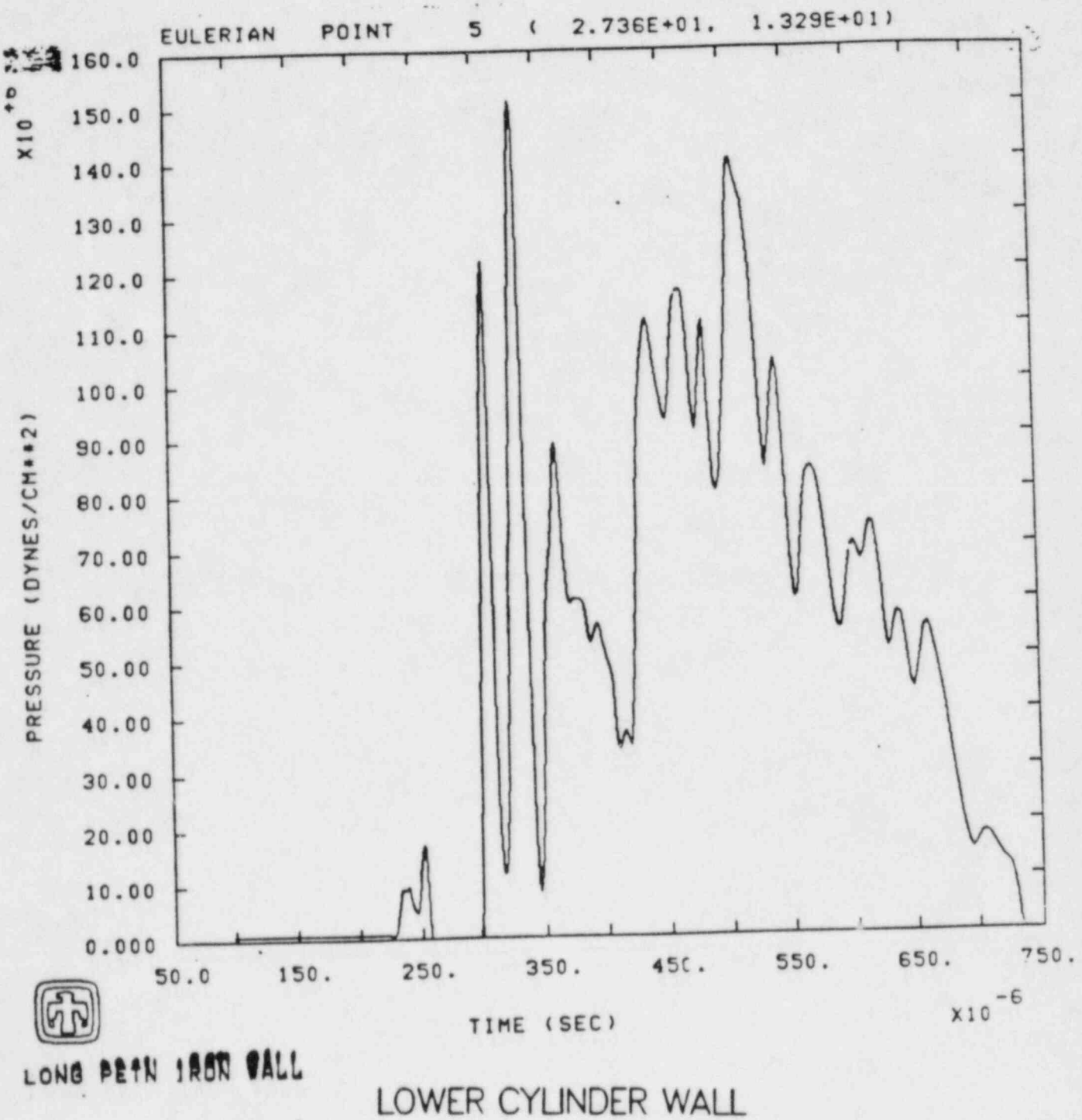

Figure 2.4 CSQ II calculation of SHE test pressure trace at lower cylinder wall position

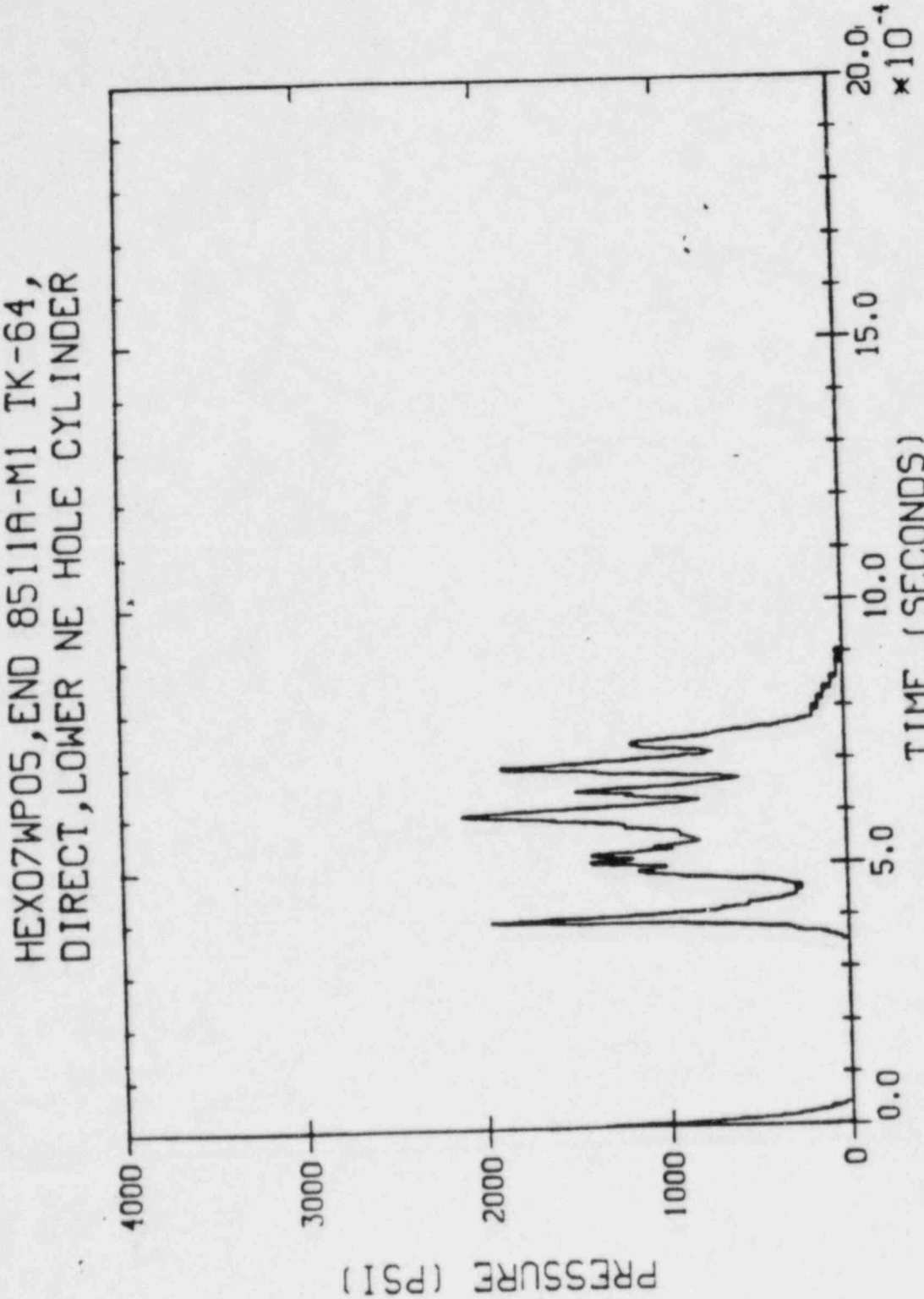

Figure 3.1 Lower wall pressure trace from HEX07 (low mount), showing individual spikes from primacord wrap.

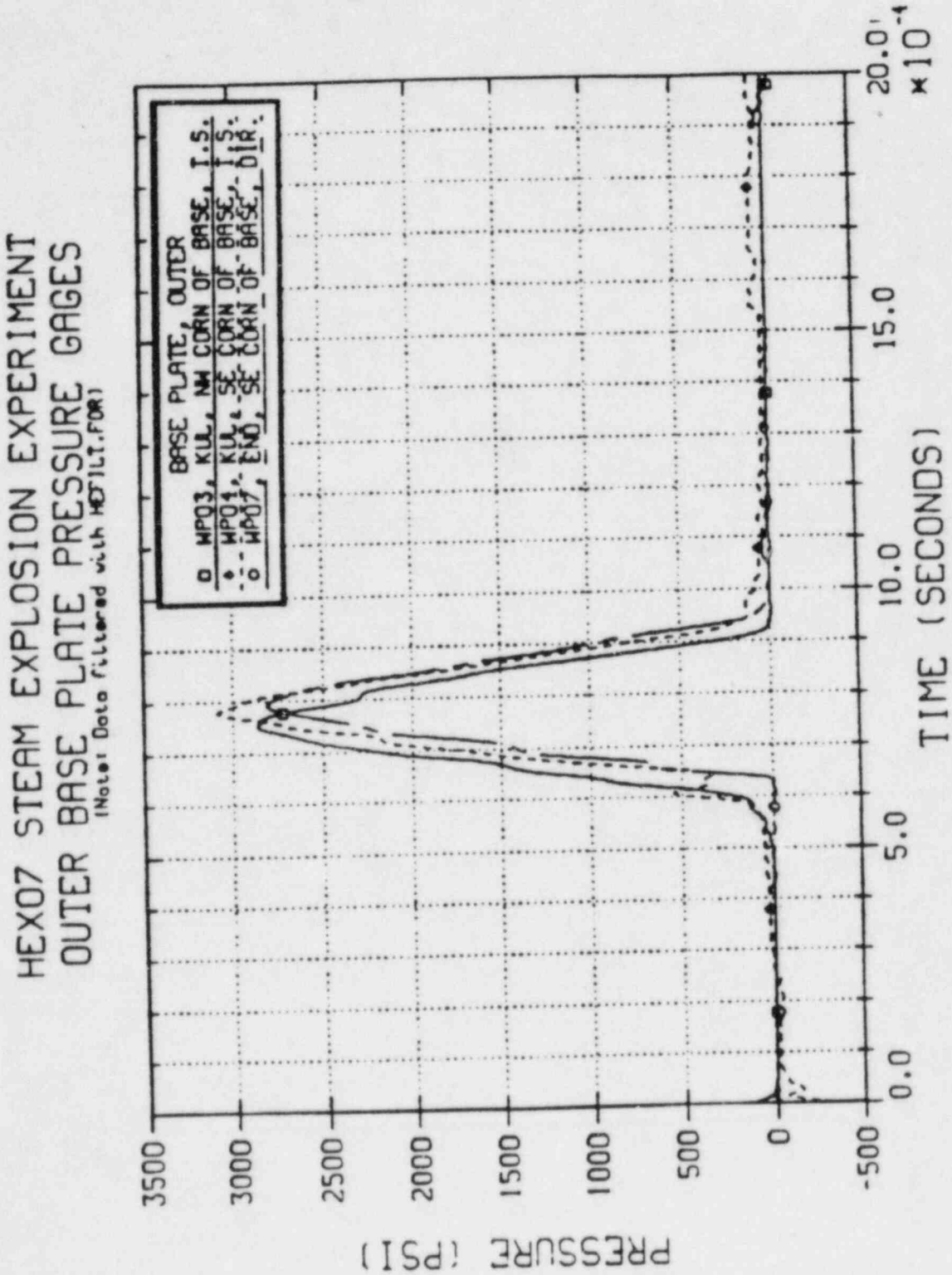

Figure 3.2 Comparison of three symmetric gage positions (outer base plate) for HEX07.

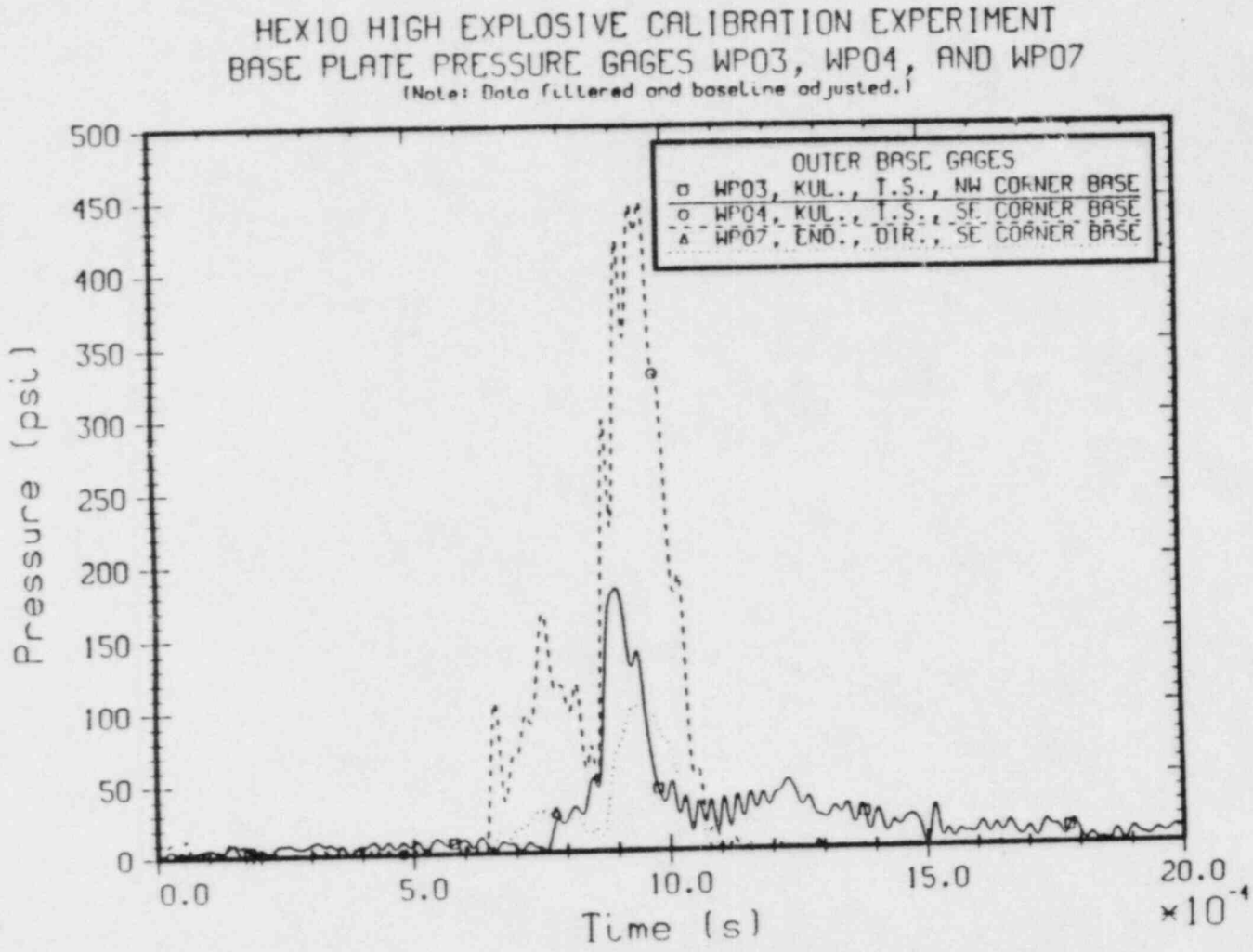

Figure 3.3 Comparison of three symmetric gage positions (outer base plate) for HEX10 lucite chamber test.

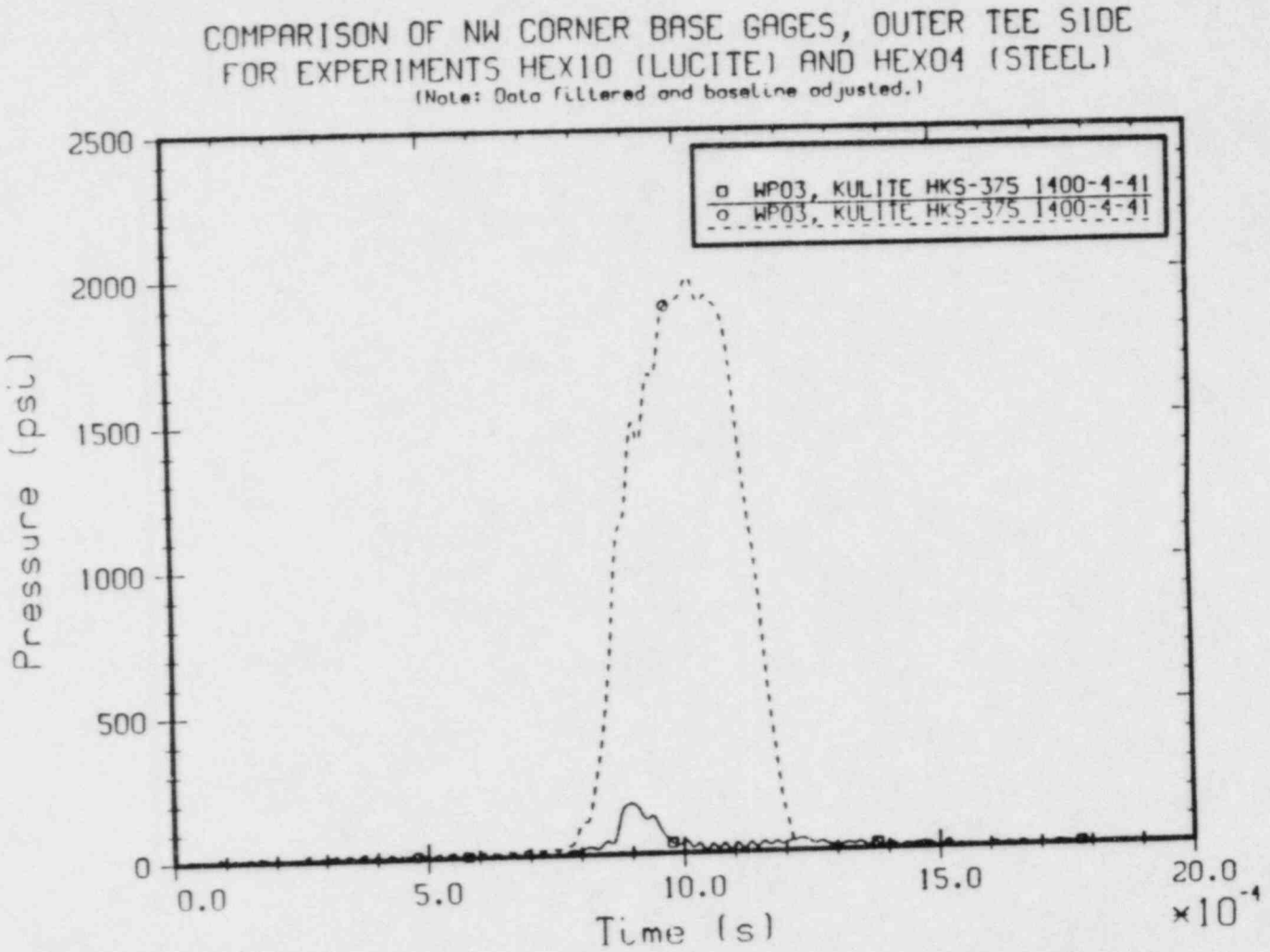

Figure 3.4 Comparison of outer base position gages in HEX07 (steel cylinder) and HEX10 (lucite chamber).

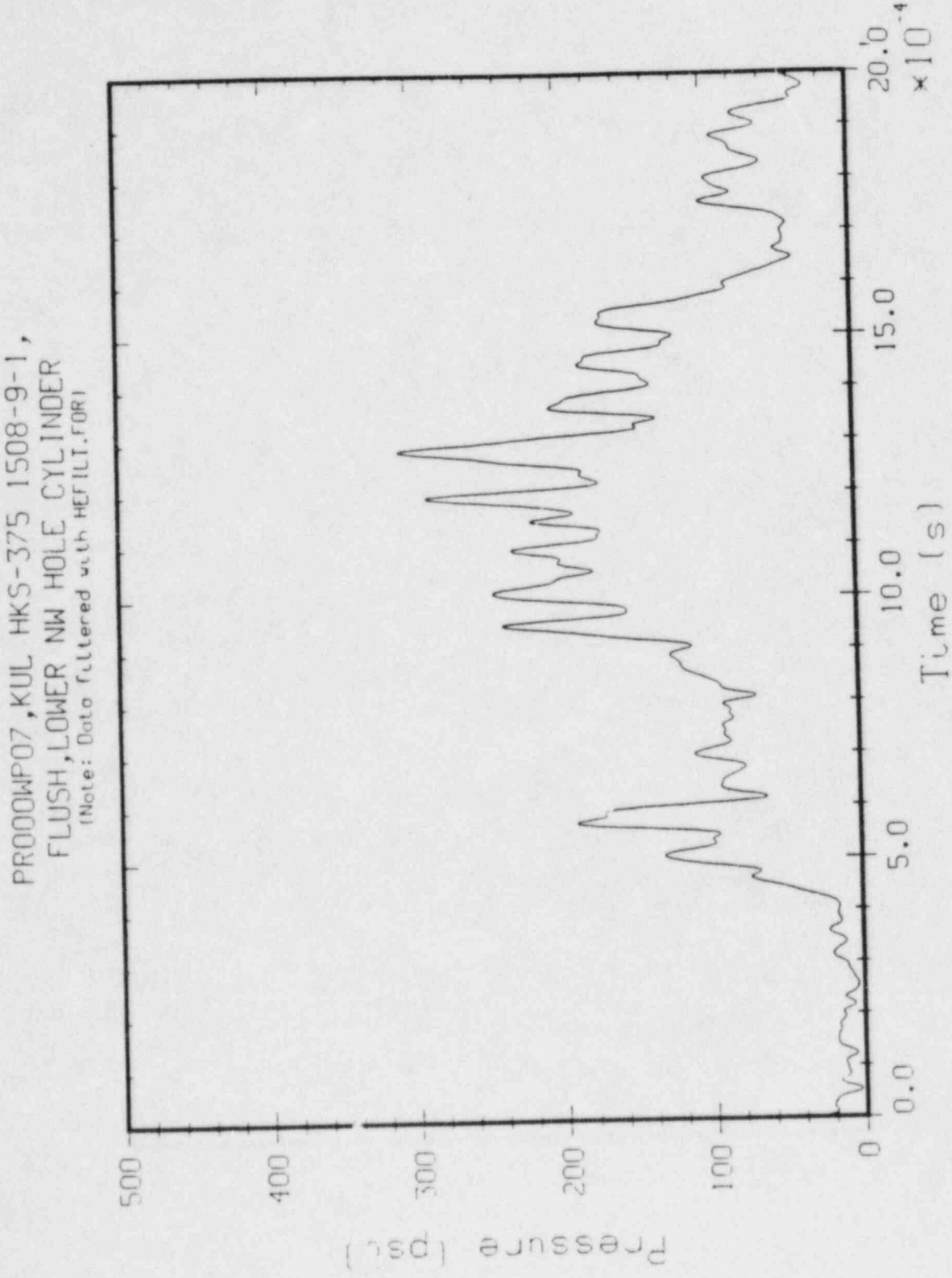

Figure 4.1 PR000 propellant test, wall-mounted gage, lower NW wall.

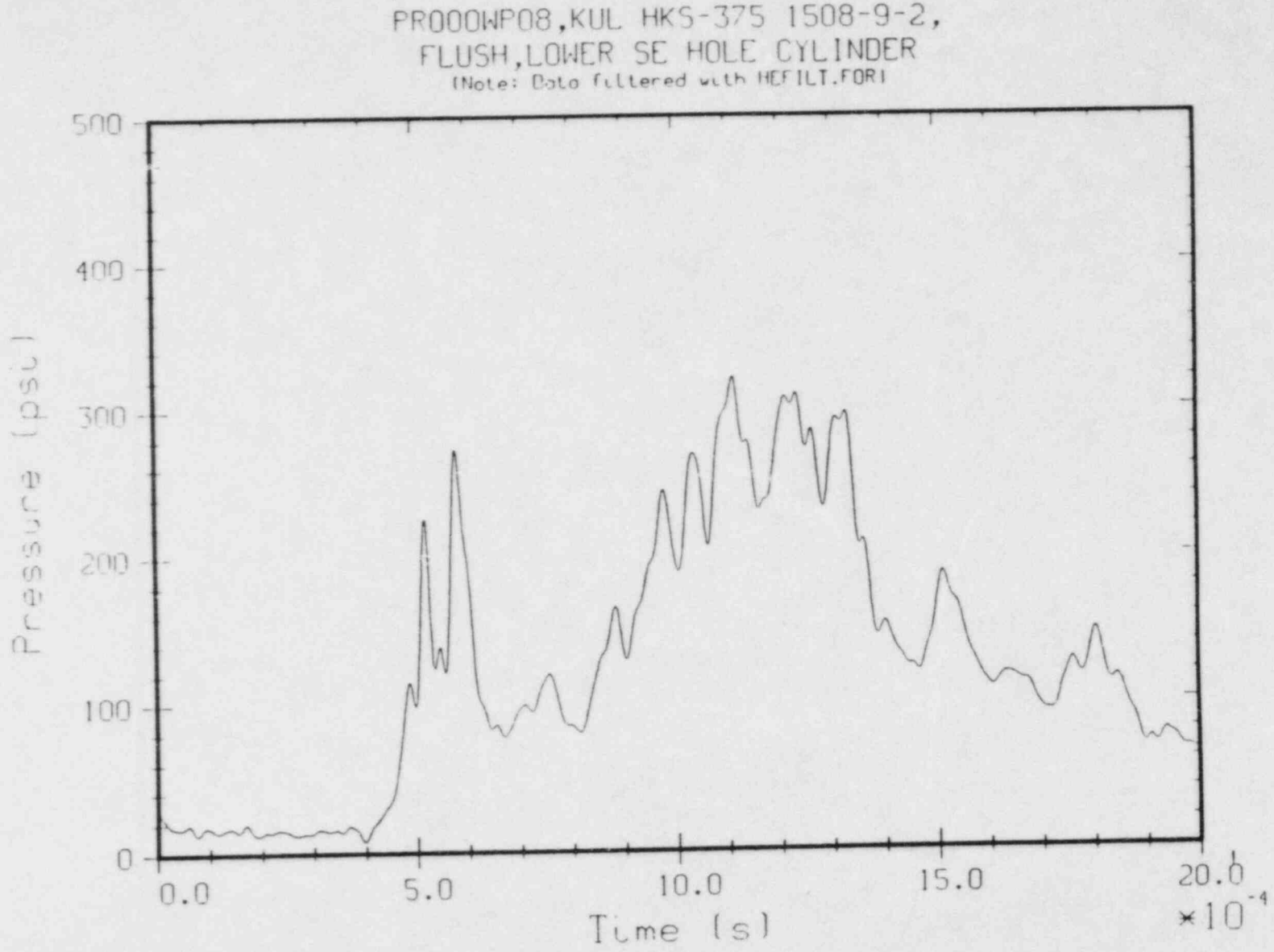

Figure 4.2 PR00 propellant test, wall-mounted gage, lower SE wall.

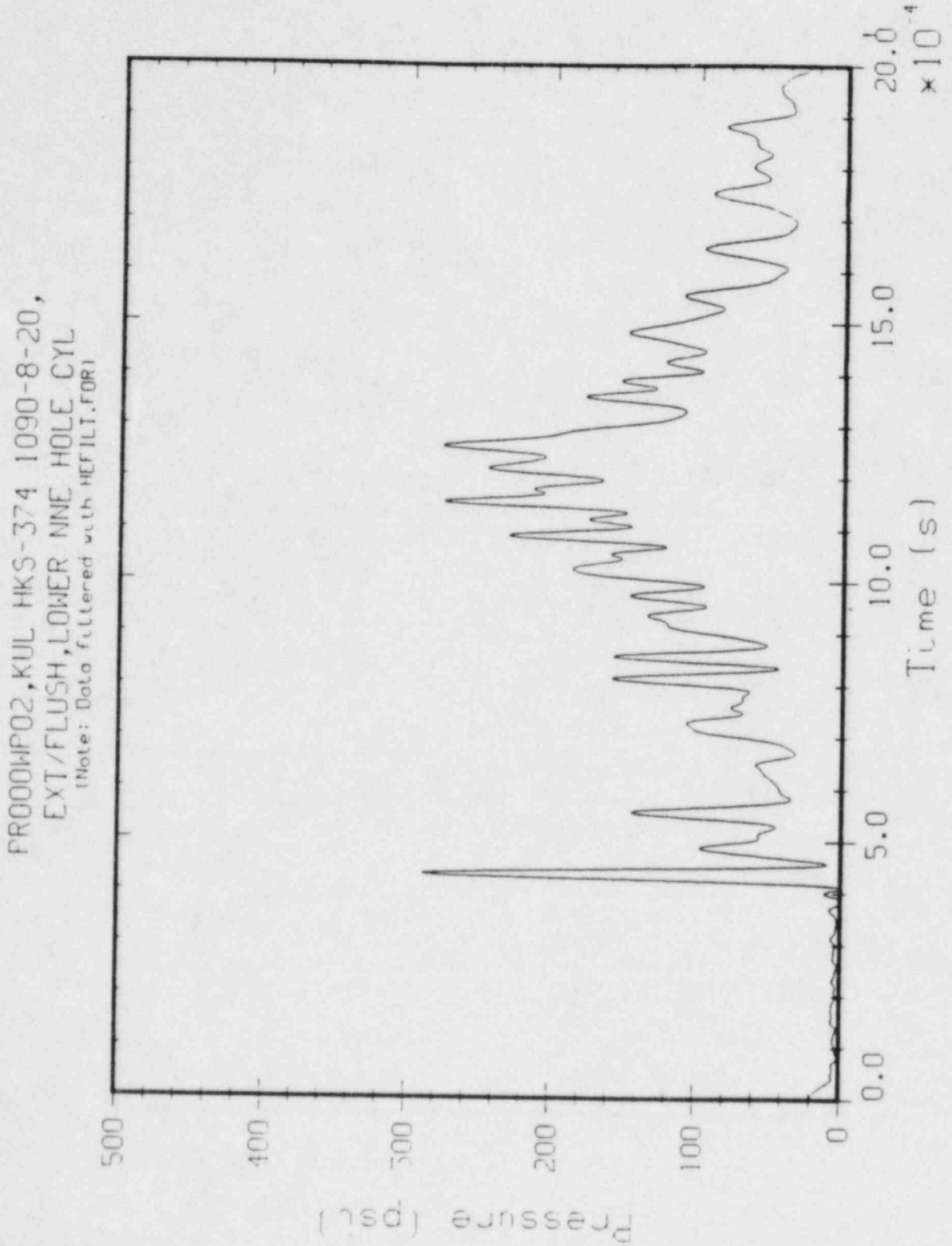

Figure 4.3 PR000 propellant test, isolation mount gage, lower NNE wall.

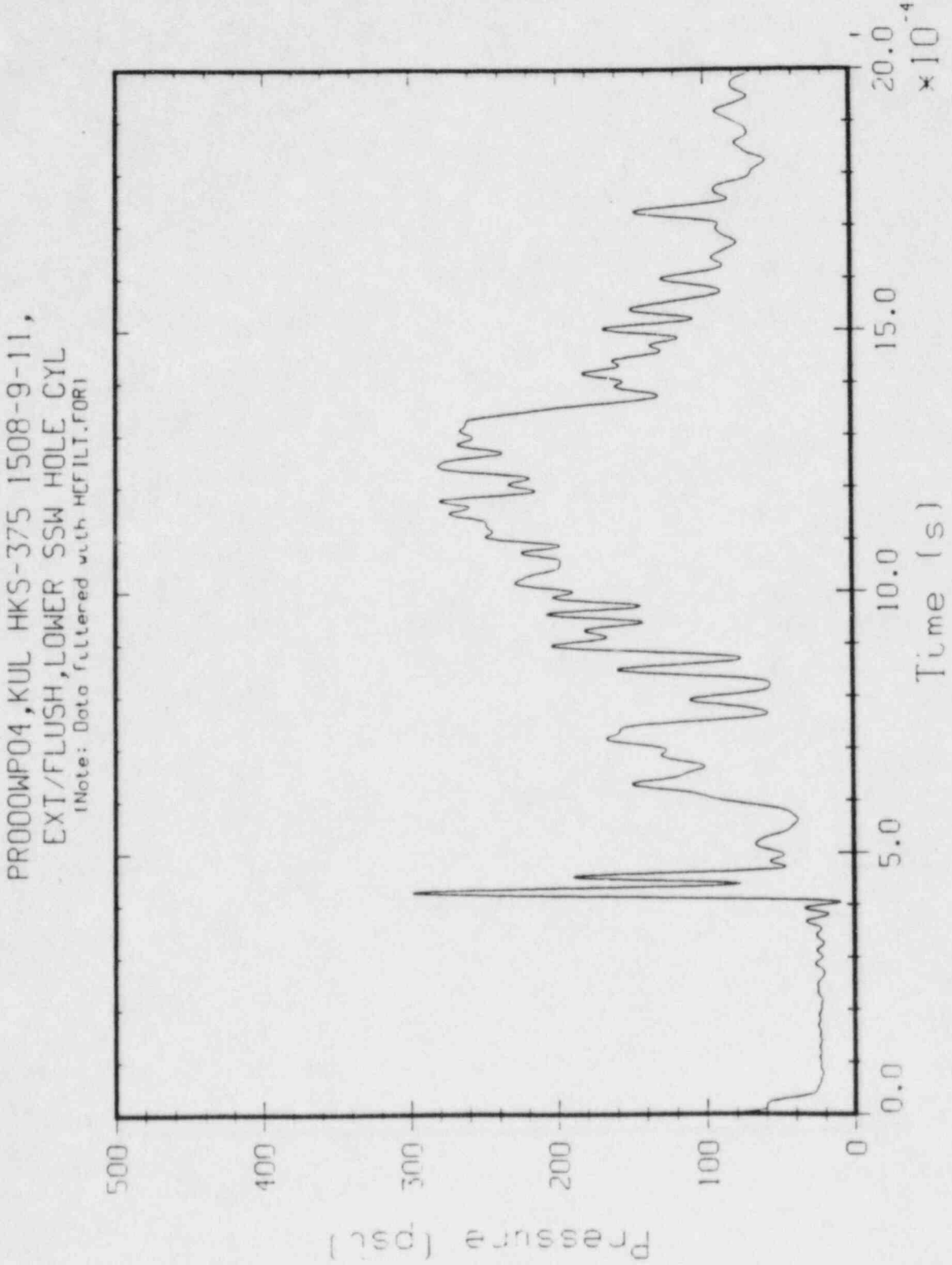

Figure 4.4 PR000 propellant test, isolation mount gage, lower SSW wall.